Multifidelity Methods for Multidisciplinary Design Under Uncertainty

by

Daniel Erik Christensen

B.S., Iowa State University (2009)

Submitted to the Department of Aeronautics and Astronautics
in partial fulfillment of the requirements for the degree of

Master of Science in Aeronautics and Astronautics

at the

MASSACHUSETTS INSTITUTE OF TECHNOLOGY

September 2012

Author .....
Department of Aeronautics and Astronautics
August 23, 2012

Certified by .....
Karen Willcox
Professor of Aeronautics and Astronautics
Thesis Supervisor

Certified by .....
Doug Allaire
Research Scientist of Aeronautics and Astronautics
Thesis Supervisor

Accepted by .....
Eytan H. Modiano
Professor of Aeronautics and Astronautics
Chair, Graduate Program Committee

Multifidelity Methods for Multidisciplinary Design Under Uncertainty

by

Daniel Erik Christensen

Submitted to the Department of Aeronautics and Astronautics
on August 23, 2012, in partial fulfillment of the
requirements for the degree of
Master of Science in Aeronautics and Astronautics

Abstract

For computational design and analysis tasks, scientists and engineers often have available many different simulation models. The output of each model has an associated uncertainty that is a result of the modeling process. This uncertainty is referred to as model discrepancy and is defined as the deviation of the model output relative to the "true" physical value. The design process typically begins with computationally inexpensive, lower fidelity models and advances to the higher fidelity models as knowledge of the design space is acquired.

Previous research has developed a Bayesian-based multidisciplinary design optimization (BMDO) framework for conducting multifidelity design with uncertainty. Fidelity level is associated with the magnitude of model discrepancy. Model selection is determined by apportioning design uncertainty to the disciplines to identify key contributors. As fidelity level increases, information from the lower fidelity models is used to complement the higher fidelity results through information fusion instead of being discarded, a more traditional approach in multifidelity optimization.

This research expands on the previously developed BMDO framework by investigating the effects of interdisciplinary coupling and model correlation on the design process. Uncertainty in the coupling variables is introduced to the BMDO framework. Multifidelity models tend to be founded on similar underlying physics and numerical methods. As a result, the model output from different fidelities may exhibit non-negligible correlation. This research demonstrates that exclusion of model correlation and uncertainty due to interdisciplinary coupling may result in underestimates of the uncertainty in design quantities of interest.

Thesis Supervisor: Karen Willcox
Title: Professor of Aeronautics and Astronautics

Thesis Supervisor: Doug Allaire
Title: Research Scientist of Aeronautics and Astronautics

Acknowledgments

The research presented in this thesis was made possible through the helpfulness and understanding of a great many people. I would first like to thank my advisor Professor Karen Willcox for her patience and enthusiasm. Karen's helpfulness and expertise helped immensely as my research progressed. Karen was always available to answer my questions or offer a sanity check when necessary. I would also like to thank Dr. Doug Allaire for his helpfulness on the technical aspects of the research project. My questions were endless—but so was his patience.

The members of the Aerospace Computational Design Laboratory (ACDL) contributed immeasurably to the success of my research and overall experience at MIT. Andrew March was always available to answer questions about optimization and provide advice. Chelsea He helped me learn how to "drink from the fire hose" while taking the course 6.431. Hemant Chaurasia was always there to provide advice and encouragement. His calmness was always reassuring. Sergio Amaral proved to be a valuable friend and classmate. The members of ACDL were always available for advice, technical questions, and a smile when needed most.

I'd also like to thank my family and friends for their support and patience during my adventures here at MIT. I wasn't always able to visit frequently and my studies often required my full attention. However, they were always understanding and their encouragement never wavered.

Finally, I would like to thank David Kordonowy, Nathan Fitzgerald, and Justin McClellan at Aurora Flight Sciences for their technical support on the project. My never-ending emails asking questions about their physics models were always answered quickly and kindly. Their patience was resolute and expertise invaluable.

This work was supported by the AFOSR STTR Program, Program Manager Dr. Fahroo, Technical Monitor Dr. Camberos, under contract FA9550-09-C-0128.

Contents

List of Figures

List of Tables

Chapter 1

Introduction

Multidisciplinary design optimization (MDO) involves the simultaneous, collaborative consideration of multiple disciplines and their interactions during an optimization process. Traditional MDO methods employ computationally inexpensive low fidelity models early in the design process to explore the design space. Higher fidelity models are used when sufficient confidence in the design has been gained to warrant the increased computational expense. Bayesian-based MDO (BMDO) considers the inclusion of uncertainty in the design process and provides a method for fidelity management to identify the level of model fidelity necessary to achieve a desired level of uncertainty. The research presented in this thesis extends the previously developed BMDO techniques by investigating the effects of interdisciplinary coupling and model correlation on the design process.

1.1 Motivation for Bayesian MDO

Multifidelity optimization methods were developed to harness the computationally inexpensive nature of simple models and accuracy of complicated models. These methods employ simple models for design space exploration to identify regions of the design space that are of particular interest relative to the optimization goals, quantified via the performance metric. Once confidence in the design is gained, computational resources may be allocated to higher fidelity models, targeting portions of

the design where improvements in accuracy are needed most.

Recent developments in MDO have sought to preserve previously acquired low fidelity information to avoid information loss or neglect. Instead of supplanting low fidelity information once high fidelity information is available, information from multiple fidelities is synthesized by weighting the information relative to the confidence in the respective sources. The synthesized result may provide a level of accuracy greater than the inputs. These advances have been achieved via the inclusion of Bayesian statistics into the MDO process, resulting in a "Bayesian-based approach for representing, fusing and managing information of varying fidelity within a multidisciplinary aerospace vehicle design environment" [5].

Numerical simulation is often employed to predict the behavior of real-world phenomena. Unfortunately, these computational models never exactly predict real-world behavior. The discrepancy may be due to the complexity of the physics involved, the modeling assumptions employed, and/or the stochastic nature of the problem. While simple models provide computationally inexpensive estimates of the performance metric, the uncertainty of the results is potentially large. If the uncertainty of the simple models is too high, the results may not be trusted or useful, no matter how computationally cheap the model.

The level of uncertainty in the performance metric is a result of the uncertainty generated from the disciplines and varies with model fidelity. An inverse relationship typically occurs between model fidelity and uncertainty; that is, higher fidelity models tend to have lower associated uncertainties. This further explains the push for higher fidelity as the design process advances—uncertainty in the design must be reduced via the incorporation of more accurate, albeit more computationally expensive, models.

Bayesian-based multidisciplinary design optimization (BMDO) employs two techniques to achieve an improved reduction in performance metric uncertainty as the design process progresses: the management of model fidelity and fusion of information from multiple sources. Model fidelity management is accomplished via the apportionment of performance metric uncertainty due to each discipline. This technique identifies disciplines with disproportionately large contributions to the performance

metric uncertainty, pinpointing key opportunities for uncertainty reduction. The result is identification of which discipline will cause the largest reduction in performance metric uncertainty if the model fidelity is incremented.

This technique enables confident use of lower fidelity tools via a quantified procedure for identifying when a higher fidelity tool is necessary. This method avoids wasting computational resources due to increasing fidelity too early in the design process, when the design is still nebulous, or a lack of uncertainty reduction from the excessive use of low accuracy information.

Information fusion improves uncertainty estimates by synthesizing information from multiple fidelities. Even low fidelity estimates of the performance metric with high uncertainty may have unique information that may be used in conjunction with higher fidelity estimates of the performance metric to produce an uncertainty estimate smaller than either of the inputs. This enables higher fidelity information to be complemented by lower fidelity information instead of merely supplanting lower fidelity results. This preservation of information may improve computational efficiency by incorporating more previously computed or readily generated information, potentially reducing the number of expensive higher fidelity model calls required to achieve to a specific level of uncertainty.

1.2 Literature Review

The BMDO method proposed in Reference [5] applied the work in estimation theory presented in Ref. [12] to multifidelity, multidisciplinary conceptual design. Uncertainty produced as a consequence of the modeling is of particular interest. Kennedy et al. proposed the definition of this model uncertainty in Ref. [21] as the discrepancy in the output of a model with respect to some "true" value. Later work termed the uncertainty as "model discrepancy", which is maintained throughout this paper [16, 22].

As defined in the previous BMDO literature, uncertainty estimates from models of different fidelity level are combined via information fusion as proposed by Winkler

et al. in Ref. [39]. Other methods to accomplish this task include Bayesian model averaging, the adjustment factors approach, and the modified adjustment factors approach as discussed in Refs. [24, 27, 30, 31].

A variety of approaches have been applied towards multifidelity optimization. March and Alexandrov et al. discussed methods for multifidelity optimization using a calibration approach in which higher fidelity results replaced lower fidelity information instead of combining the information [2, 3, 26]. Forrester et al. and Booker et al. have conducted optimization on an expensive black-box model by creating a surrogate to act as a lower fidelity model [8, 13, 14, 15]. Other methods have employed the use of an additive or multiplicative correction between the lower and higher fidelity models [20, 25]. The higher fidelity model is occasionally sampled and the correction between the models is updated. Gradient-free multifidelity optimization has been investigated in Refs. [26] and [28]. Alexandrov et al. proved local convergence using the trust-region method for multifidelity optimization [2, 3]. Multifidelity optimization with a strict hierarchy of models based on model fidelity has been investigated by Choi et al. [9]. The formulation of the BMDO method is sufficiently general to be applicable to problems that lack a model fidelity hierarchy.

1.3 Objectives

The objectives of this work advance previous BMDO research by developing methods to incorporate disciplinary coupling and model correlation. The previously developed BMDO method assumed each discipline may be evaluated independent of the others. That is, no interdisciplinary dependencies, referred to as coupling, exist. The output of each discipline serves as input into a performance block, which calculates the performance metric. This research advances the BMDO method via the inclusion of interdisciplinary coupling. Output from each discipline may serve as input into the performance block and/or another discipline. This opens the possibility of feedback loops between disciplines and greatly complicates the estimation of performance metric uncertainty and attribution of this uncertainty to its sources (the disciplines).

Models of varying fidelity for a given discipline may also not be independent sources of information. Increases in fidelity may be due to additional physics being modeled or the use of finer meshes. Even though the higher fidelity models provide more accurate, less uncertain results, the output of the different fidelity models may exhibit some level of correlation. The effect of correlation on the BMDO process is investigated in this research. The effect of correlation on the information fusion step is of particular interest since the consequences affect both the management of model fidelity and estimation of performance metric uncertainty.

1.4 Outline

Chapter 2 discusses the basic BMDO method. The various aspects of the BMDO framework are discussed and a walkthrough of the BMDO method using an an aircraft design problem is conducted. Chapter 3 describes how the coupling is addressed and investigates the effects of coupling on the BMDO framework. Chapter 4 investigates model correlation and its influence on fidelity management and attribution of performance metric uncertainty to the respective disciplines. The results are summarized in Chapter 5 and recommendations for future work are proffered.

Chapter 2

Bayesian-based Multidisciplinary Optimization

The formulation and terminology for multidisciplinary design optimization are defined. The BMDO algorithm is presented and each step of the algorithm and its role are discussed in detail. The physics models used for our problem of interest are discussed and a walkthrough of the BMDO process using these models is performed.

2.1 BMDO Framework

2.1.1 MDO Formulation and Terminology

A variety of variable types are employed in the MDO methodology. Design variables are degrees of freedom that serve as inputs to the disciplines and performance block. Design variables are the properties being optimized or modified to create the design. A collection of design variables is referred to as a design vector. Design variables are denoted by the symbol x.

Coupling variables are outputs of one discipline and inputs into another discipline. These variables are represented by the symbol y_{AB} where the first and second subscripts denote the source and destination disciplines, respectively. Disciplinary outputs are variables that are outputs of a discipline and inputs into the performance

block. Disciplinary outputs are denoted by z_{AP}, where the subscripts represent the variable is an output of discipline A and an input to performance block P. It is possible for a variable to be both a coupling variable and disciplinary output. That is, a particular output for a discipline may be an input into both another discipline and the performance block. The term "performance metric" is generalized by referring to a specific output of the performance block as a "quantity of interest".

A summary of these variable types is shown in Table 2.1. It is important to note for later discussion that lowercase and uppercase symbols denote deterministic and random variables, respectively.

Variable Type	Symbol	Source	Destination
Design Variables	x	Optimizer, User	Disciplines, Performance
Coupling Variables	y_{AB}	Discipline A	Discipline B
Disciplinary Output	z_{AP}	Discipline A	Performance P
Quantity of Interest	q	Performance	n/a

Table 2.1: Description of Variables for MDO methodology

A diagram displaying a general two-discipline MDO flowchart is shown in Figure 2-1. A design vector is generated from the optimizer, user, or other source and is passed directly to the disciplines and/or performance block. The arrow denoting design variables being passed to the performance block is excluded for clarity. The disciplines, shown here as 'Module A' and 'Module B', accept design and coupling variables from other disciplines as inputs, and output coupling variables and disciplinary outputs. The performance block accepts disciplinary outputs and design variables as inputs and calculates the quantity of interest, an output of the performance block. It may be observed that the dual-coupling between the two disciplines creates a potential for a feedback loop.

2.1.2 BMDO Algorithm

The steps for a single BMDO iteration are shown in Algorithm 1 [5]. The process starts with all disciplines using their lowest fidelity model. The BMDO method consists of multiple iterations and continues until the BMDO termination criteria

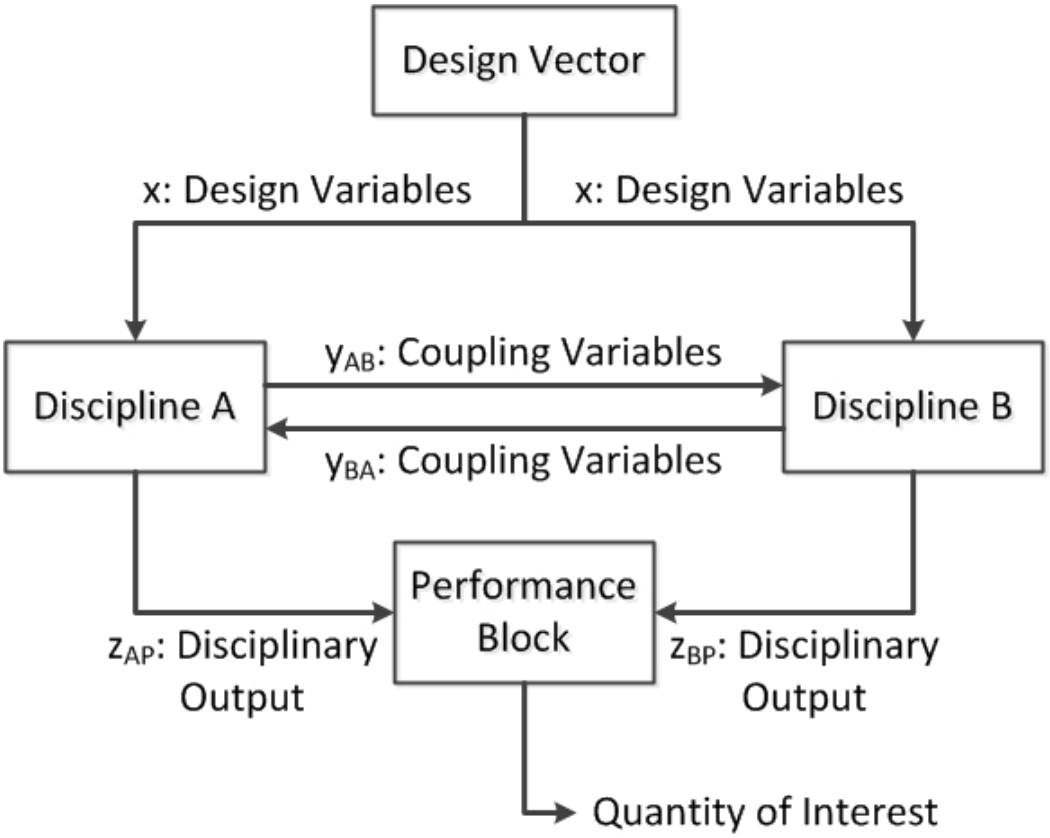

Figure 2-1: Flowchart for General MDO Formulation

are satisfied as shown in Step 5. Each step is explained in detail in the subsequent subsection.

Algorithm 1 Bayesian-based Multidisciplinary Design Optimization Iteration

1. Given an initial design, conduct optimization until convergence criteria are satisfied.
2. Quantify uncertainty of disciplinary outputs.
3. Conduct information fusion on disciplinary outputs for disciplines in which a lower fidelity model exists.
4. Estimate quantity of interest and associated uncertainty.
5. Determine if BMDO termination criteria are satisfied. If yes, exit algorithm.
6. Conduct global sensitivity analysis to apportion quantity of interest uncertainty to source disciplines.
7. Identify primary contributors to quantity of interest uncertainty, increase model fidelity of these disciplines.

2.1.3 Discussion of BMDO Algorithm

The BMDO method iteration is comprised of multiple steps. This section individually discusses each of the steps in detail.

Step 1: Optimization

Optimization is conducted to locate designs with improved performance metrics. These tools traverse the design space using some determined search algorithm which may include: gradient descent, random/genetic search, etc. The search continues until convergence criteria are satisfied or the optimizer is unable to progress any further.

Step 2: Disciplinary Output Uncertainty

The uncertainty associated with the disciplinary output must be quantified and applied to the deterministic disciplinary output values. This and previous research in the BMDO method consider only uncertainty due to model discrepancy. Model discrepancy is defined as the deviation of a particular model's output from the unknown "true" value. This error or deviation associated with the output of a model may be due to missing physics, modeling assumptions, and/or the stochastic nature of the phenomenon being modeled. The uncertainty due to model discrepancy is modeled via some arbitrary function of the discipline or performance block's input and/or output.

A flowchart of the application of uncertainty due to model discrepancy is shown in Figure 2-2. Disciplinary output with uncertainty is generated by adding model discrepancy to the deterministic disciplinary output values, z_{AP}. Model discrepancy is denoted by ϵ with subscripts matching the disciplinary output to which the discrepancy is being applied. Uncertainty due to model discrepancy is generated by sampling a normal distribution with the calculated variance and zero mean.

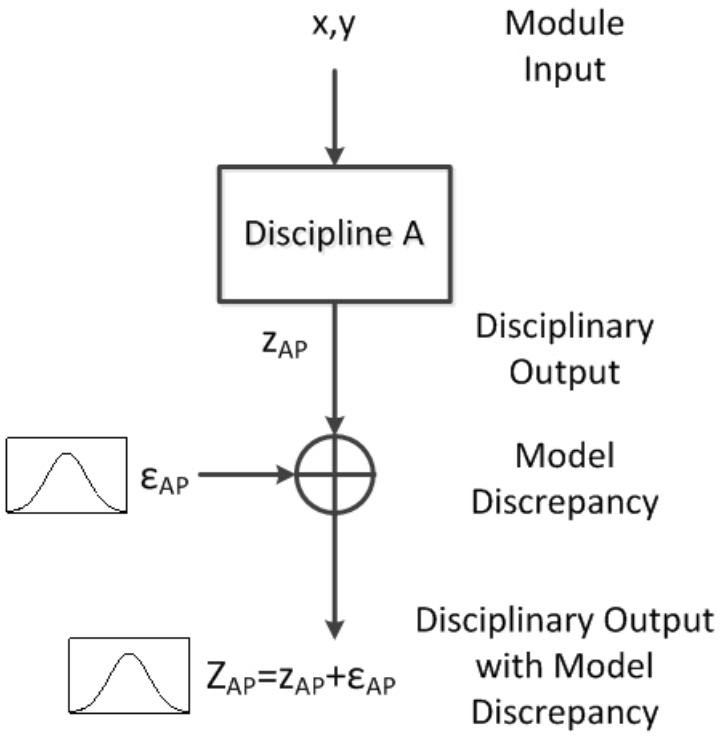

Figure 2-2: Method for Applying Uncertainty Due to Model Discrepancy

Step 3: Information Fusion

If one or more of the disciplines has a lower fidelity model available, an information fusion step occurs; otherwise, the algorithm proceeds onto the next step. Information fusion combines knowledge from multiple sources to produce a single improved synthesized result. This process starts with the estimation of the disciplinary output values and associated uncertainty using multiple models of varying fidelity. Information fusion is conducted on each discipline individually and all fidelity models for a given discipline are evaluated using the same design and coupling variable inputs. Once multiple estimates of the disciplinary output values and uncertainty are generated, the estimates are synthesized to form an improved estimate of both the disciplinary values and uncertainty. This process extracts information from multiple sources, resulting in a synthesized estimate of the uncertainty that is smaller than any of the inputs.

This method preserves previously generated results to enable lower fidelity information to inform higher fidelity results rather than simply being supplanted once

higher fidelity results are available. In addition, this method incorporates results from computationally inexpensive lower fidelity models to improve the uncertainty estimates of a higher fidelity models.

Equations 2.1 and 2.2 are used to calculate the fused mean and variance for a particular disciplinary output [39]. These equations assume normal distributions as inputs and output a fused normal distribution. The numerical subscripts identify whether the variable corresponds to the first or second input. The subscript "F" identifies the fused variable. Mean values are denoted by μ and variance by σ^2. The correlation coefficient is denoted by ρ and quantifies the correlation between the two input sources. Previous research applied the assumption of independent models ($\rho = 0$) and employed the simplified formulas shown in Equations 2.3 and 2.4.

$$\mu_F = \frac{\left(\sigma_2^2 - \rho\sigma_1\sigma_2\right)\mu_1 + \left(\sigma_1^2 - \rho\sigma_1\sigma_2\right)\mu_2}{\sigma_1^2 + \sigma_2^2 - 2\rho\sigma_1\sigma_2} \tag{2.1}$$

$$\sigma_F^2 = \frac{\left(1-\rho^2\right)\sigma_1^2\sigma_2^2}{\sigma_1^2 + \sigma_2^2 - 2\rho\sigma_1\sigma_2} \tag{2.2}$$

$$\mu_F = \frac{\sigma_2^2\mu_1 + \sigma_1^2\mu_2}{\sigma_1^2 + \sigma_2^2} \tag{2.3}$$

$$\sigma_F^2 = \frac{\sigma_1^2\sigma_2^2}{\sigma_1^2 + \sigma_2^2} \tag{2.4}$$

The uncorrelated fusion equation for the mean (Eq. 2.3) is simply the variance-weighted average of the inputs. That is, if a large discrepancy exists between the variances of the inputs, the mean of the input with the smaller variances will be weighted more heavily. If one of the inputs has zero variance, the fused mean will be identical to the mean of the input with zero variance.

If the inputs have identical variance, the fused mean will be the arithmetic average of the inputs and the fused variance will be one half of the input variance. Fusion may be conducted on more than two distributions by first fusing two input distributions to generate a single fused distribution. A third input may then be fused with the first

fused distribution to generate a new fused distribution. This process may proceed indefinitely.

Step 4: Quantity of Interest Uncertainty

Once the mean and variance of the disciplinary outputs for all disciplines have been calculated from Steps 2 and 3, the acquired normal distributions are sampled using Latin Hypercube sampling. This method starts by randomly generating a large number of samples of the disciplinary output. The samples are each fed into the performance block, which is subsequently evaluated. The result is a large collection of calculated values for the quantity of interest which may be used to generate estimates of the mean and variance of the quantity of interest.

Step 5: Check Termination Criteria

Once the termination criteria for the BMDO method are satisfied, the algorithm terminates. These criteria may take on a variety of forms including: a maximum number of fidelity level increments or an allowable level of uncertainty in the quantity of interest. Once the uncertainty in the quantity of interest is below the specified allowable level, the algorithm terminates and no additional fidelity increments are necessary. It is also possible for the algorithm to proceed until no higher fidelity models are available, i.e. no additional sources of information are available to further reduce the quantity of interest uncertainty.

Step 6: Global Sensitivity Analysis

The BMDO framework employs a variance-based global sensitivity analysis (GSA) to attribute uncertainty in the quantity of interest to the sources. Since all uncertainty is assumed to be derived from model discrepancy, all uncertainty in the quantity of interest may be traced back to the source discipline or an interaction of source disciplines.

Sensitivity indices are defined as the percentage of quantity of interest variance that is caused by a given source. Uncertainty that is due purely to one discipline

is called the main effect and is represented via main sensitivity indices. Uncertainty due to interactions of multiple disciplines is referred to as an interaction effect and is denoted by interaction sensitivity indices. The total effect of a particular discipline is denoted via total sensitivity indices and considers all sources of uncertainty involving the specified discipline—including both main and interaction effects.

The BMDO framework employs the Sobol' method to apportion the variance in the quantity of interest to the sources [18, 37]. This method starts with two independent $M \times N$ matrices of random numbers, where M is the number of samples and N is the total number of disciplinary outputs from all disciplines. The first matrix is denoted by C and the second by D. A third set of matrices, E_i is generated by copying the matrix D and replacing all columns corresponding to disciplinary outputs of discipline i with the respective columns of matrix C. Next, the performance block is evaluated for each sample in the C, D, and E matrices to produce vectors of estimated quantity of interest values, represented by q_C, q_D, and q_{E_i} as shown in Equation 2.5. Each evaluated sample corresponds with a single entry in the quantity of interest vectors. Finally, Equations 2.7 and 2.8 are used to calculate to main and total sensitivity indices, respectively, for discipline i.

For two disciplines, only a single interaction term exists. As a result, all uncertainty not already attributed to either discipline via main effects is considered to be the result of disciplinary interactions. The equation for the interaction sensitivity index, S_I, is shown in equation 2.9. The disciplines A and B are designated via their respective subscripts.

$$q_C = f\left(C\right), \quad q_D = f\left(D\right), \quad q_{E_i} = f\left(E_i\right) \tag{2.5}$$

$$f_0^2 = \left(\frac{1}{N}\sum_{j=1}^{N} q_C^{(j)}\right)^2 \tag{2.6}$$

$$S_i = \frac{q_C \cdot q_{E_i} - f_0^2}{q_C \cdot q_C - f_0^2} \tag{2.7}$$

$$S_{T_i} = 1 - \frac{q_D \cdot q_{E_i} - f_0^2}{q_C \cdot q_C - f_0^2} \tag{2.8}$$

$$S_I = 1 - S_A - S_B \tag{2.9}$$

The Sobol' method operates by sampling and resampling data, then comparing the calculated quantity of interest vectors. The matrix C is considered the sampled data and matrix D the resampled data. To calculate the sensitivity indices for discipline i, all disciplinary outputs from the other disciplines are resampled while the disciplinary outputs corresponding with discipline i are simply sampled. This is the creation of matrix E_i. Equations 2.7 and 2.8 estimate the variance of the quantity of interest due to the disciplinary output of discipline i relative to the overall variance considering all disciplinary outputs from all disciplines. The effects of the disciplinary outputs from discipline i are isolated by the scalar products. The effects due to disciplinary outputs in modules except i are random due to the resampling and these effects will tend to zero as the number of samples increases. This leaves only the effects of the disciplinary outputs of discipline i left. A detailed description regarding this method is available in Ref. [33].

The discipline with the largest main sensitivity index has the largest contribution to quantity of interest uncertainty. This discipline is a candidate for an increase in model fidelity level since it may result in the largest achievable uncertainty reduction. Figure 2-3 shows a flowchart for the GSA method. To calculate the sensitivity indices for discipline A, ϵ_{AP} is sampled and ϵ_{BP} is resampled. Conversely, to calculate the sensitivity indices of discipline B, ϵ_{BP} is sampled and ϵ_{AP} is resampled.

Step 7: Increment Model Fidelity

The management of model fidelity level is a crucial component of the BMDO method. Increasing fidelity too early in the design process is computationally expensive and risky. Computational resources may be wasted exploring undesirable regions of the design space. Increasing model fidelity too late in the design process stalls the reduc-

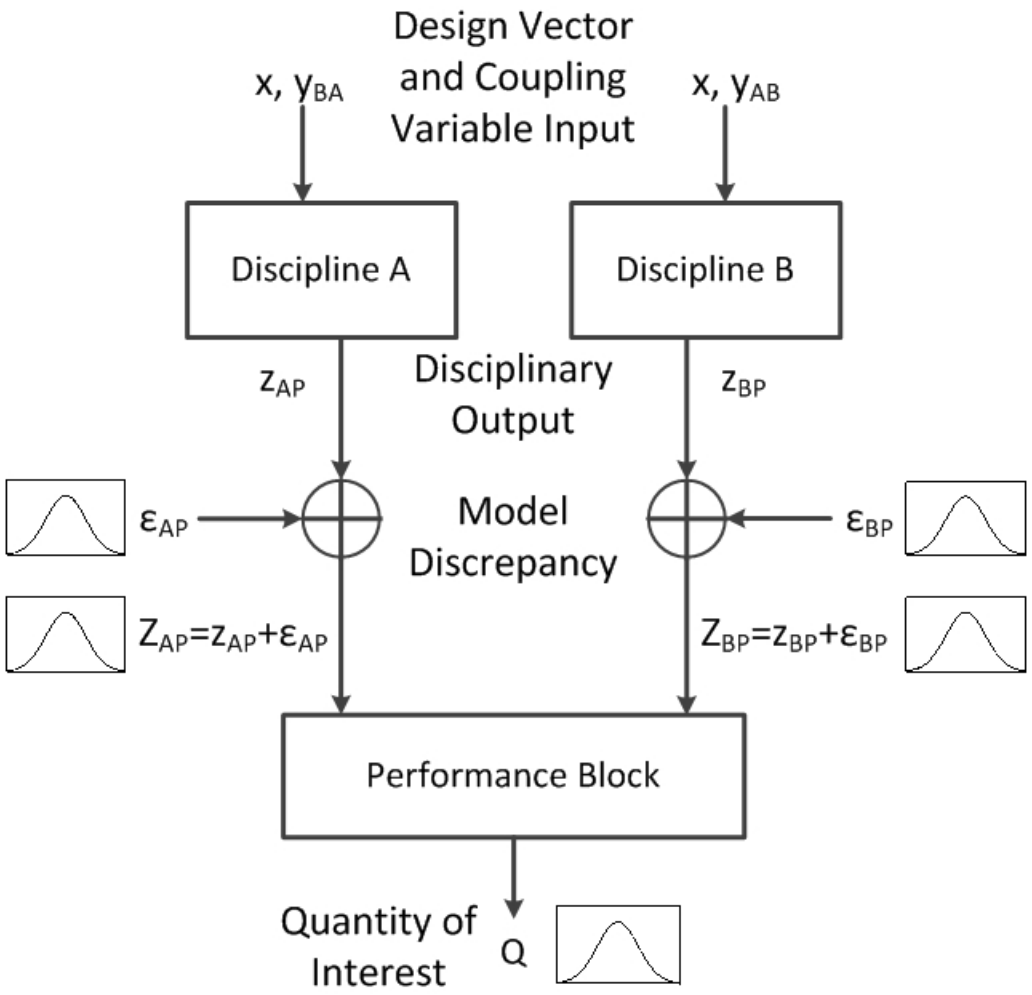

Figure 2-3: Problem Setup for Coupled System Global Sensitivity Analysis

tion of uncertainty as the design process proceeds without the necessary information from the higher fidelity models.

After the completion of the Step 6 and the calculation of main sensitivity index for each discipline, the discipline with the largest main sensitivity index is increased in fidelity level while all other disciplines are held at their current fidelity level. This method only increases fidelity level when necessary to achieve further reduction in uncertainty and only increases fidelity for the discipline with the largest contribution to overall uncertainty in the quantity of interest. This avoids unnecessarily increasing fidelity level for disciplines which would provide little reduction in uncertainty.

2.2 Physics Models

Our problem of interest is the design of a medium-altitude, long-endurance unmanned aerial vehicle (UAV) with minimal fuel burned in order to complete a specified mission. Two disciplinary models were developed: structures and aeropropulsion [23]. Each model has two fidelity levels [17]. The performance block has a single fidelity level.

2.2.1 Structures Module

The structures model considers four components of the aircraft: the fuselage, wing, and horizontal/vertical tail surfaces. It is assumed the wing and tail surfaces create all forces and moments for flight and control. The wing and tail are linearly tapered and swept. External fuel storage pods are attached to the wing for increased flight endurance.

The fuselage is modeled as a cylinder with a conical tail. A standard two-surface tail comprised of horizontal and vertical surfaces is considered. The fuselage is sized by the payload and avionics volumetric requirements. Both the fuselage and wing are available for fuel storage. A fixed tripod-style arrangement for landing gear is assumed. Landing gear location and heights are selected to minimize landing loads and ensure adequate ground clearance, governed by the Federal Aviation Regulations for air worthiness (FAR 23).

Internal iterations are used to close the loop between aircraft loading, structural sizing, and weight estimation. The fidelity levels are differentiated by the methods used for sizing and weight estimation.

Low Fidelity

Model outputs are primarily calculated by weight estimation using Raymer and Roskam correlations [29, 32]. The generality of these relationships enables the low fidelity model to be applicable for several classes of aircraft. This potentially aids the exploration of the design space since the model may be applicable for a wide range of possible inputs. Margins-of-safety are not considered for the low fidelity model.

Medium Fidelity

First principles are employed for sizing the primary (load-bearing) structures [40]. Weight fractions are used to estimate the mass of secondary (non-load-bearing) structures. Primary and secondary weight estimates are synthesized to form a composite estimate of the aircraft weight. Margins of safety are considered for structural strength, static margin, and balance.

2.2.2 Aeropropulsion Module

Two primary propulsive components are considered for the aeropropulsion model. The powerplant provides shaft power by consuming fuel. The propulsor generates thrust via the conversion of shaft power. The powerplant is a turbocharged four-stroke diesel engine that consumes JP-8 fuel. The propulsor is a three-bladed variable pitch operating at a constant rotational rate. The model assumes the aircraft has two engines, one located on each wing.

Both on and off-design analyses are performed for the aeropropulsion model. The engine is sized via the on-design analysis. The minimum engine power required to achieve the specified flight conditions during each segment of the flight is calculated. Engine weight is estimated based on the minimum power requirements to complete the mission. Off-design calculates maximum thrust available, throttle required for desired flight performance, and fuel consumption at any moment during the flight. These values are used to estimate mission performance.

Drag is calculated via the synthesis of multiple components of drag, including induced, parasitic, and trim drag. These calculations estimate the drag during the mission based on the aircraft geometry, empty weight, and fuel weight. Mission segments are discretized and the loads are balanced at each step. Flight speed is determined by ensuring a valid coefficient of lift while minimizing drag [1]. Changes in aircraft weight due to fuel burned is considered at each discretization step for all mission segments. An Oswald efficiency factor of 0.85 and a fixed base coefficient of drag of 0.02 are assumed. A statistical relationship between wing loading and

thrust-to-weight is used to estimate take-off distance [11].

Low Fidelity

Actuator disk theory is used to estimate the propeller thrust for a given streamtube capture area and power input from the powerplant. The powerplant assumes constant brake specific fuel consumption for all flight conditions and power settings. Thrust specific fuel consumption (TSFC) variations are due to changes in propulsive efficiency only.

Medium Fidelity

Blade element theory is used to estimate propeller thrust. Blade loading and propeller rotational speed are considered in these calculations. A turbocharged diesel engine cycle analysis is used to estimate engine performance. A simple thermodynamics model without specific heat variance due to temperature is employed. A cycle analysis is completed to calculate the necessary displacement of the engine to meet power requirements. Engine weight is estimated from correlations of total engine displacement.

2.2.3 Performance Block

The performance metric is the mass of fuel required to fly the specified mission. The Breguet range equation is used to calculate the fuel burned for the cruise and loiter segments of the mission. Cruise distance and loiter duration are constants for the problem.

2.2.4 Variables and Constraints

The problem of interest has a total of twenty-five design variables, shown in Table 2.2. Twenty-one design variables are exclusively for the structures module and two for the aeropropulsion module. The remaining two design variables are shared between both modules. Many of the design variables have been normalized or nondimensionalized.

Station positions for the wing and tail surfaces are nondimensionalized by the surface's span. Surface chords are normalized via the root chord and fuel fill ratios are normalized by total fuel volume available.

Variable	Units	Destination(s)
Wingspan	ft	Structures and Aeropropulsion
Horizontal Tail Aspect Ratio	-	Structures and Aeropropulsion
Wing Aspect Ratio	-	Structures
Wing Root Station Position	-	Structures
Wing Engine Station Position	-	Structures
Wing Pylon Station Position	-	Structures
Wing Engine Station Chord	-	Structures
Wing Pylon Station Chord	-	Structures
Wing Tip Station Chord	-	Structures
Wing Sweep Angle	deg	Structures
Horizontal Tail Root Station Position	-	Structures
Horizontal Tail Tip Station Chord	-	Structures
Horizontal Tail Sweep Angle	deg	Structures
Horizontal Tail Position	-	Structures
Vertical Tail Aspect Ratio	-	Structures
Vertical Tail Root Station Position	-	Structures
Vertical Tail Tip Station Chord	-	Structures
Vertical Tail Sweep Angle	deg	Structures
Vertical Tail Position	-	Structures
Wing Fuel Fill Ratio	-	Structures
Fuselage Fuel Fill Ratio	-	Structures
Length of Nose Ratio	ft	Structures
Length of Tail Ratio	ft	Structures
Turbocharger Pressure Ratio	-	Aeropropulsion
Propeller Radius	m	Aeropropulsion

Table 2.2: Design Variables for Aircraft Design Problem

The wing and tail surfaces have several break points. All three surfaces have root and tip breaks. The root break point designates where the surface's sweep and taper characteristics begin. The area of the surface in-board of the root break point is unswept and untapered. The tip break point marks the farthest extent from the fuselage for a particular surface. The wing also has break points for the engine and pylons (for fuel storage). Each surface has its own sweep angle that starts at the root

position. A single sweep angle is used for the wing instead of a unique sweep angle for each of three wing sections from the root to tip stations.

Figure 2-4 shows a flowchart displaying the variable flow between disciplines and the performance block for our problem. The structures module takes five coupling variables as inputs from the aeropropulsion module including: engine weight and flight speeds. The flight speeds are used for stability calculations. The structures module has ten outputs, shown in Table 2.3, which include: aircraft weight, fuel weight, planform area, fuselage surface area, horizontal tail surface area, root chord, mean chord, location of the center of gravity, location of neutral point, and horizontal tail position. The structures module calculates six constraints. Four of the constraints measure the margins of safety for the fuselage, wing, and horizontal/vertical tail surfaces. The remaining two calculate the center of gravity and neutral point to ensure a stable aircraft design.

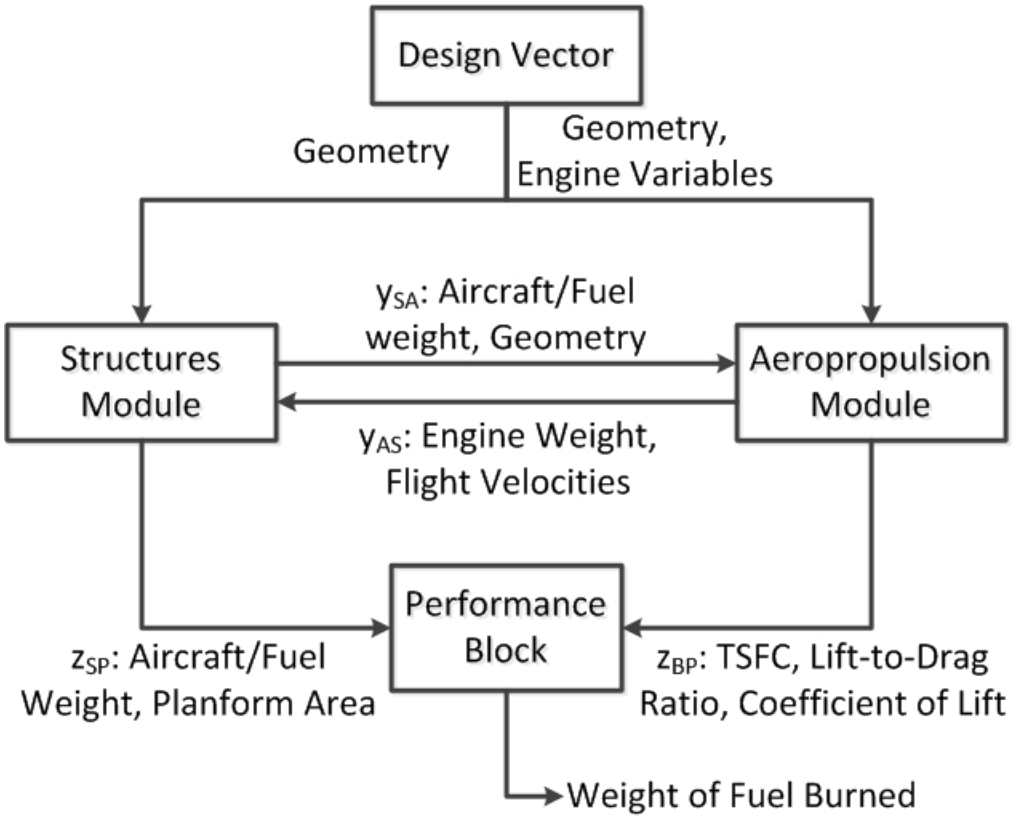

Figure 2-4: Flowchart for Aircraft Design Problem

Variable	Units	Source	Destination(s)
Aircraft Weight	lbm	Structures	Aeropropulsion and Performance
Weight of Fuel On-Board	lbm	Structures	Aeropropulsion and Performance
Planform Area	ft^2	Structures	Aeropropulsion and Performance
Fuselage Wetted Area	ft^2	Structures	Aeropropulsion
Root Chord	ft	Structures	Aeropropulsion
Mean Chord	ft	Structures	Aeropropulsion
Horizontal Tail Planform Area	ft^2	Structures	Aeropropulsion
Position of Center of Gravity	ft	Structures	Aeropropulsion
Position of Neutral Point	ft	Structures	Aeropropulsion
Position of Horizontal Tail	ft	Structures	Aeropropulsion
Engine Weight	lbm	Aeropropulsion	Structures
Cruise Speed	kts	Aeropropulsion	Structures
Dive Speed	kts	Aeropropulsion	Structures
Stall Speed	kts	Aeropropulsion	Structures
Maximum Operating Speed	kts	Aeropropulsion	Structures
Cruise TSFC	hr^{-1}	Aeropropulsion	Performance
Loiter TSFC	hr^{-1}	Aeropropulsion	Performance
Cruise Lift-to-Drag Ratio	-	Aeropropulsion	Performance
Loiter Lift-to-Drag Ratio	-	Aeropropulsion	Performance
Cruise Lift Coefficient	-	Aeropropulsion	Performance
Loiter Lift Coefficient	-	Aeropropulsion	Performance

Table 2.3: Coupling Variables and Disciplinary Outputs for Aircraft Design Problem

The aeropropulsion module has ten coupling variable inputs from the structure module which provide important geometric values for the aerodynamics analysis. There are eleven outputs of the aeropropulsion module, including: engine weight, flight speeds, TSFCs, lift-to-drag ratios, and lift coefficients. Two of the eight aeropropulsion constraints ensure sufficient excess engine power to reach cruise altitude and maintain a specified minimum climb rate. Another four constraints set bounds on the allowable coefficient of lift and Mach numbers. The final two aeropropulsion constraints ensure sufficient thrust is generated to maintain flight during the loiter and cruise segments of the mission.

The performance block takes nine inputs from the structures and aeropropulsion modules: aircraft weight, fuel weight, planform area, TSFCs, lift-to-drag ratios, and

lift coefficients. The output of the performance block are the weight of fuel burned in order to complete the desired mission. The single constraint for the performance block ensures the weight of fuel on-board meets or exceeds the weight of fuel required to perform the specified mission.

2.3 Application of BMDO

This section briefly discusses the application of the BMDO process to our problem. Problem-specific information regarding the BMDO process is provided and a walk-through of the BMDO method is completed using the BMDO methodology developed by previous research. Disciplinary coupling and model correlation are not considered for this section but will be discussed in the later chapters.

2.3.1 Problem-Specific Information

Optimization

Optimization is conducted using Matlab's "fmincon" function, a constrained nonlinear minimization algorithm. This routine uses gradient-based optimization methods to minimize the performance metric. Optimization proceeds until a minimum is located within the specified stopping conditions or if the function fails to find a minimum. Due to the complexity of our problem and the tendency of gradient methods to locate local minima, many starting points were considered as a way to search a greater portion of the design space. The settings used for optimization are shown in Table 2.4 and are elements of Matlab's"optimset" feature.

Setting	Description	Value
Algorithm	Algorithm for optimization	Interior-point
TolFun	Convergence tolerance for objective function	10^{-3}
TolCon	Convergence tolerance for constraints	10^{-3}
TolX	Convergence tolerance for design variables	10^{-5}
MaxFunEvals	Maximum number of function evaluations	10^{4}
DiffMinChange	Minimum step size for finite differencing	10^{-3}

Table 2.4: Optimization Settings

A fixed-point iteration was used to converge the coupling variable values. This method evaluates each discipline in succession and updates the coupling variable values after each disciplinary evaluation. This procedure proceeds until the change in coupling variables is less than a specified tolerance. A maximum of twenty fixed-point iterations were allowed and the convergence tolerance was 10^{-5}.

Uncertainty Estimation

Uncertainty in model outputs due to model discrepancy was assumed to have a standard deviation that is proportional to the deterministic value at the designated design point. The standard deviation of the uncertainty for low and medium fidelity models were 15% and 10% of the deterministic value, respectively. All uncertainty due to model discrepancy is assumed to be Gaussian in accordance with the maximum entropy method [19].

After the completion of steps 2 and 3 of the BMDO algorithm, normal distributions for each of the disciplinary outputs have been generated. Matlab's Latin hypercube sampling function "lhsdesign" is used to generate a total of $50,000$ samples. Next, the performance block is evaluated for each sample. The mean and variance of the quantity of interest are estimated from the evaluations of the performance block.

2.3.2 First Iteration

The initial design was determined by sampling the disciplines and selecting the feasible point with the best performance metric (lowest mass of fuel burned during specified mission). Figure 2-5 shows the feasible initial design. The starting design is similar in appearance to existing medium-altitude, long-endurance UAVs. Both the structures and aeropropulsion modules employ low fidelity models. The BMDO method is set to terminate when no additional fidelity increases are available. Table A.1 in Appendix A contains the values of the design variables for the design vectors generated during the BMDO walkthrough. The associated coupling variables and disciplinary outputs for these design vectors are available in Table A.2.

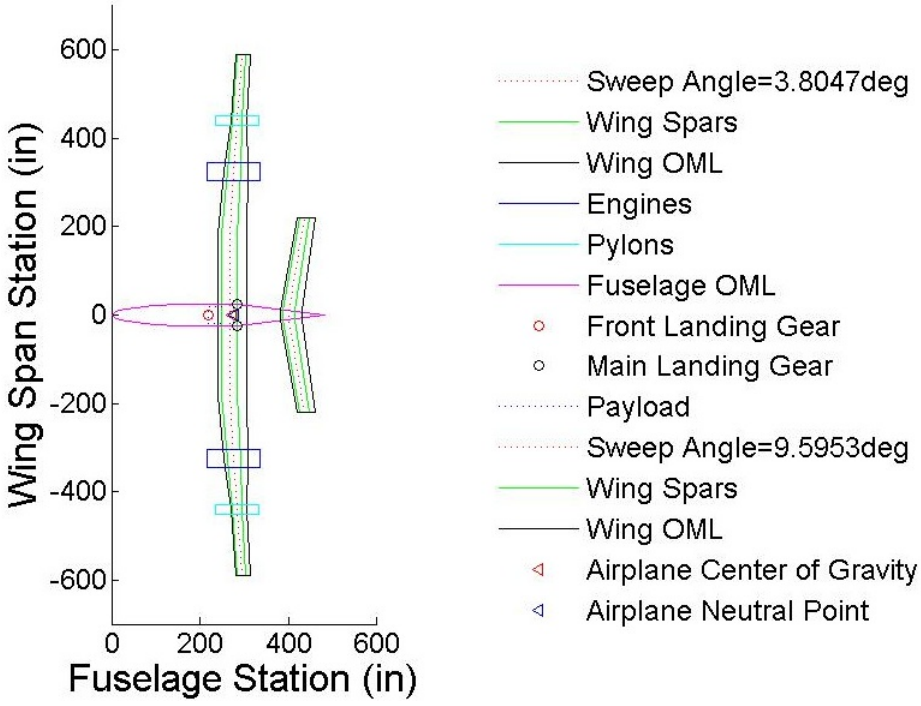

Figure 2-5: Initial Feasible Design

Step 1: Optimization

Starting at the feasible initial design, optimization was completed to produce the optimized design shown in Figure 2-6. The size of the aircraft has decreased considerably, most notably the length of the fuselage and wing chord. The wing has become slightly more swept and the aspect ratio of the wing has increased. The horizontal tail surface has decreased in both area and span.

Step 2: Disciplinary Output Uncertainty

The deterministic values of the disciplinary output and their associated standard deviation due to uncertainty are shown in Table 2.5.

Step 3: Information Fusion

No lower fidelity models are available for either the structures or aeropropulsion module. As a result, no information fusion is performed and the algorithm proceeds onto the next step.

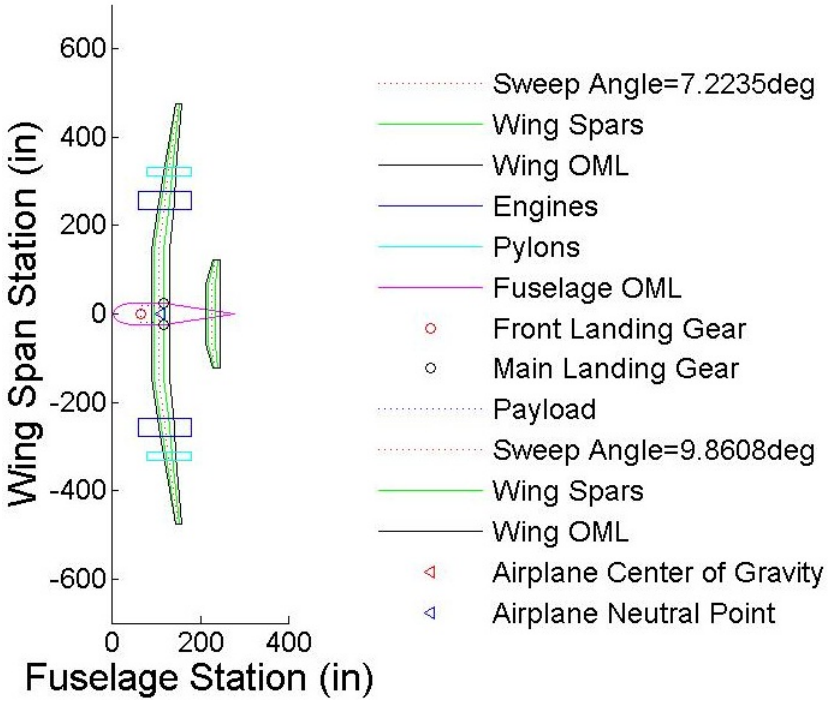

Figure 2-6: Optimized Design for First Iteration

Variable	Units	Deterministic Value	Standard Deviation
Aircraft Weight	lbm	3989	598.4
Weight of Fuel On-Board	lbm	1349	202.3
Planform Area	ft^2	214.0	32.11
Cruise TSFC	hr^{-1}	0.167	0.025
Loiter TSFC	hr^{-1}	0.105	0.16
Cruise Lift-to-Drag Ratio	-	22.87	3.43
Loiter Lift-to-Drag Ratio	-	30.13	4.52
Cruise Lift Coefficient	-	0.543	0.081
Loiter Lift Coefficient	-	0.943	0.141

Table 2.5: Deterministic Disciplinary Output Values and Uncertainty for First Iteration

Step 4: Quantity of Interest Uncertainty

The disciplinary output distributions calculated in step 2 are sampled and the performance block is evaluated. The result is a mean of 1359 lbm with a standard deviation of 269.2 lbm for the quantity of interest.

Step 5: Check Termination Criteria

The termination criteria are not satisfied; higher fidelity models exist for both the structures and aeropropulsion modules. The algorithm proceeds onto the next step.

Step 6: Global Sensitivity Analysis

The results of the first global sensitivity analysis are shown in Table 2.6 and visualized with a pie diagram.

Sensitivity Index	Value
Structures Main	0.44
Aeropropulsion Main	0.55
Structures Total	0.45
Aeropropulsion Total	0.55
Interaction	0.01

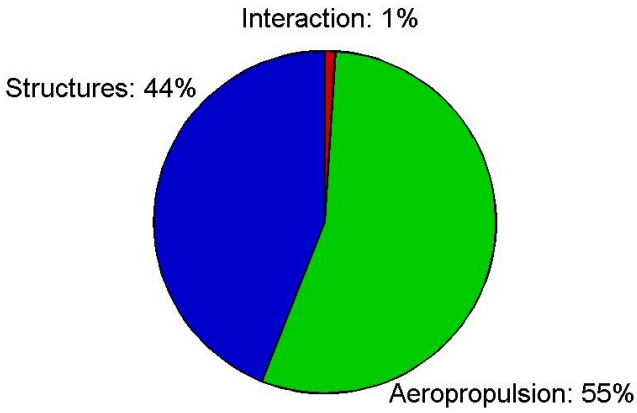

Table 2.6: Results of First Global Sensitivity Analysis

Step 7: Increment Model Fidelity

The aeropropulsion module is the largest contributor to the quantity of interest uncertainty. As a result, the aeropropulsion model fidelity level is incremented to medium while the structures model remains at low fidelity.

2.3.3 Second Iteration

Step 1: Optimization

Optimization starts with the optimized design from the previous iteration. The low fidelity structures and medium fidelity aeropropulsion models are used for optimization. The new optimized design is shown in Figure 2-7. Wing sweep has decreased

slightly. Wing span and chord have increased, providing more volume in the wing for fuel storage. The length of the fuselage has increased.

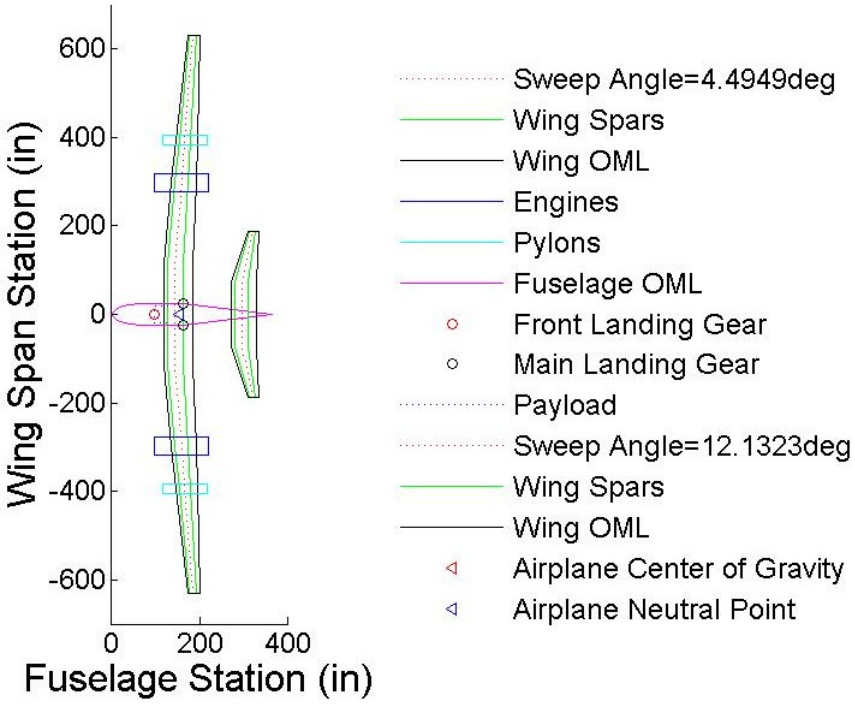

Figure 2-7: Optimized Design for Second Iteration

Step 2: Disciplinary Output Uncertainty

The deterministic values of the disciplinary output and associated standard deviation due to model discrepancy are shown in Table 2.7.

Step 3: Information Fusion

Information fusion is conducted on the disciplinary output distributions calculated in the previous step. Disciplinary output distributions are generated by evaluating the low fidelity aeropropulsion model with the same design and coupling variable inputs as the current fidelity case. Step 2 is repeated for the low fidelity aeropropulsion results to convert the deterministic output of the low fidelity aeropropulsion model into a distribution that considers model discrepancy. The resultant distribution from the low fidelity model is fused with the results from the medium fidelity model as

Variable	Units	Deterministic Value	Standard Deviation
Aircraft Weight	lbm	5529	829.3
Weight of Fuel On-Board	lbm	2115	317.3
Planform Area	ft^2	452.5	67.9
Cruise TSFC	hr^{-1}	0.103	0.010
Loiter TSFC	hr^{-1}	0.107	0.011
Cruise Lift-to-Drag Ratio	-	28.21	2.82
Loiter Lift-to-Drag Ratio	-	24.02	2.40
Cruise Lift Coefficient	-	0.991	0.099
Loiter Lift Coefficient	-	0.625	0.062

Table 2.7: Deterministic Disciplinary Output Values and Uncertainty for Second Iteration

shown in Figure 2.8. Since a lower fidelity structures model is not available, the disciplinary outputs from the structures module are not fused. The column labeled "current fidelity" denotes results generated from current fidelity models, which were used during the optimization for this iteration. For the second iteration, this includes low fidelity structures and medium fidelity aeropropulsion.

Variable	Units	Low Fidelity	Current Fidelity	Fused Mean
Structures Fidelity	-	Low	Low	-
Aeropropulsion Fidelity	-	Low	Med.	-
Aircraft Weight	lbm	5529	5529	5529
Weight of Fuel On-Board	lbm	2116	2116	2116
Planform Area	ft^2	452.5	452.5	452.5
Cruise TSFC	hr^{-1}	0.112	0.103	0.106
Loiter TSFC	hr^{-1}	0.113	0.107	0.109
Cruise Lift-to-Drag Ratio	-	28.22	28.22	28.22
Loiter Lift-to-Drag Ratio	-	23.97	24.02	24.00
Cruise Lift Coefficient	-	0.991	0.991	0.991
Loiter Lift Coefficient	-	0.623	0.625	0.624

Table 2.8: Results of First Information Fusion

Step 4: Quantity of Interest Uncertainty

Sampling of the fused disciplinary output distributions from Step 3 and subsequent evaluation of the performance block leads to a new mean of 2135 lbm and standard

deviation of 339.9 lbm for the mass of fuel burned. The increase in standard deviation of the quantity of interest despite a model fidelity increase is due to an increase in the values of the deterministic disciplinary outputs. Since model discrepancy is modeled as a relative fraction of the deterministic mean, the uncertainty associated with the disciplinary outputs has increased proportionately.

Step 5: Check Termination Criteria

The termination criteria are not satisfied; a higher fidelity model exists for the structures module. The algorithm proceeds onto the next step.

Step 6: Global Sensitivity Analysis

Global sensitivity analysis results for the second iteration are shown in Table 2.9.

Sensitivity Index	Value
Structures Main	0.66
Aeropropulsion Main	0.33
Structures Total	0.67
Aeropropulsion Total	0.33
Interaction	0.00

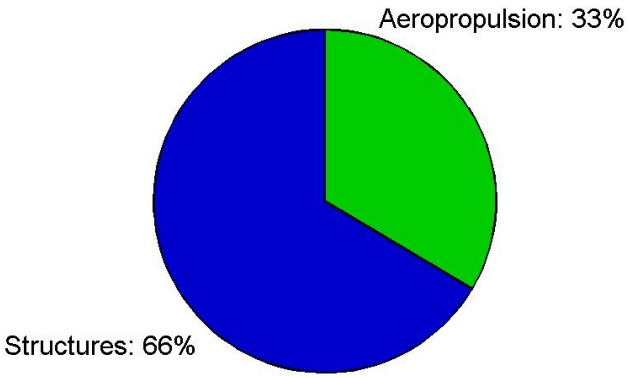

Table 2.9: Results of Second Global Sensitivity Analysis

Step 7: Increment Model Fidelity

A majority of the uncertainty in the quantity of interest is due to the structures module. As a result, the fidelity level of the structures model is increased to medium while the aeropropulsion model remains at medium fidelity.

2.3.4 Third Iteration

Step 1: Optimization

The design from the previous iteration is used as the starting point for optimization, which is completed with both disciplines using medium fidelity models. The new optimized design is shown in Figure 2-8. The sweep of the wing has further decreased and the fuselage has been elongated. The wing continues to provide significant volume for fuel storage. In addition, the fuel volume of the fuselage has increased.

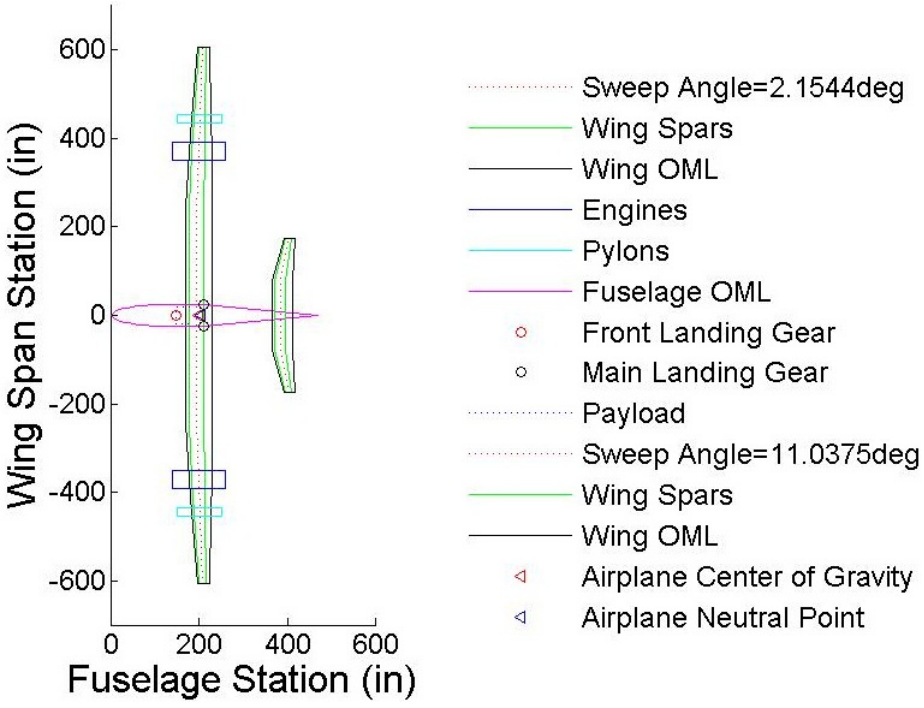

Figure 2-8: Optimized Design for Third Iteration

Step 2: Disciplinary Output Uncertainty

The deterministic values of the disciplinary output and associated standard deviation due to uncertainty are shown in Table 2.10.

Step 3: Information Fusion

Information fusion is conducted on the disciplinary output distributions calculated in the previous step. Both the structures and aeropropulsion modules have lower fidelity

Variable	Units	Deterministic Value	Standard Deviation
Aircraft Weight	lbm	5358	535.8
Weight of Fuel On-Board	lbm	2052	205.2
Planform Area	ft^2	435.2	43.52
Cruise TSFC	hr^{-1}	0.103	0.010
Loiter TSFC	hr^{-1}	0.107	0.011
Cruise Lift-to-Drag Ratio	-	27.75	2.78
Loiter Lift-to-Drag Ratio	-	23.88	2.39
Cruise Lift Coefficient	-	0.999	0.100
Loiter Lift Coefficient	-	0.629	0.063

Table 2.10: Deterministic Disciplinary Output Values and Uncertainty for Third Iteration

models available. As a result, information fusion will be conducted on both modules. Current fidelity results are generated with both structures and aeropropulsion employing medium fidelity models.

The low fidelity models are evaluated using the same design and coupling variable inputs as the medium fidelity models. Uncertainty is applied to the deterministic output and the low and medium fidelity distributions are fused to produce fused distributions. The mean values of the fused distributions are shown in Table 2.11.

Variable	Units	Low Fidelity	Current Fidelity	Fused Mean
Structures Fidelity	-	Low	Med.	-
Aeropropulsion Fidelity	-	Low	Med.	-
Aircraft Weight	lbm	5328	5358	5349
Weight of Fuel On-Board	lbm	1974	2053	2027
Planform Area	ft^2	435.2	435.2	435.2
Cruise TSFC	hr^{-1}	0.112	0.103	0.106
Loiter TSFC	hr^{-1}	0.114	0.107	0.109
Cruise Lift-to-Drag Ratio	-	27.76	27.76	27.76
Loiter Lift-to-Drag Ratio	-	23.83	23.88	23.86
Cruise Lift Coefficient	-	0.999	0.999	0.999
Loiter Lift Coefficient	-	0.627	0.629	0.628

Table 2.11: Results of Second Information Fusion

Step 4: Quantity of Interest Uncertainty

The fused disciplinary output distributions result in mean and standard deviation estimates of $2081\,lbm$ and $229.5\,lbm$, respectively, for the quantity of interest.

Step 5: Check Termination Criteria

The termination criteria are satisfied; neither the structures nor aeropropulsion module have a higher fidelity models available. The algorithm is complete. If higher fidelity models were available, the algorithm would proceed onto the fourth iteration.

2.3.5 Summary of BMDO Walkthrough

Three iterations of the BMDO method were conducted. The fidelity level of the aeropropulsion and structures modules were each incremented once. A final estimate of the mass of fuel burned to achieve the specified mission is $2081\,lbm$ and the associated uncertainty has a standard deviation of $229.5\,lbm$. The uncertainty in the quantity of interest has been reduced by 14.75% as a result of the increases in model fidelity level and information fusion steps.

Chapter 3

Disciplinary Coupling

The outputs of a particular discipline may not be functions of only the design variables and instead may use variables calculated in other disciplines. This interdisciplinary coupling creates a loop between the disciplines that may have consequences if ignored, i.e. if the disciplines are treated as independent from each other. This section discusses how coupling is addressed and its effect on the BMDO framework. The BMDO walkthrough is completed with the effects of coupling considered and the differences from the basic BMDO walkthrough are discussed.

3.1 Including Coupling in the BMDO Framework

All outputs of the disciplines have associated uncertainty due to model discrepancy regardless of the destination of the outputs. That is, outputs are uncertain whether they are disciplinary output, coupling variables, or both. Treating coupling variables as deterministic neglects a source of uncertainty: uncertainty due to coupling variable inputs.

Previous work was conducted on a problem of interest with uncoupled disciplines. Each discipline accepted a deterministic design vector as input and generated deterministic disciplinary outputs. The disciplinary outputs became random variables when uncertainty due to model discrepancy was applied to the deterministic values. The consideration of coupling variables and their associated uncertainty was unnec-

essary. Our problem of interest includes interdisciplinary coupling. Consideration of coupling variable uncertainty causes the deterministic coupling variables to now be random variables. As a result, the input to the disciplines may now include deterministic design variables and random variables for coupling.

The addition of model uncertainty may further increase the variance of the output for the nondeterministic case. That is, some of the uncertainty in a particular discipline's output is due not only to the model discrepancy of that discipline, but also due to model discrepancy of other disciplines via coupling. As a result, considering coupling variable uncertainty may increase the uncertainty of the disciplinary outputs which may in turn increase the variance of the quantity of interest. Exclusion of this extra source of uncertainty may result in the underestimation of uncertainty for the quantity of interest.

A rigorous consideration of coupling uncertainty requires that variable closure be resolved. Consider the general MDO formulation shown in Figure 2-1. Uncertainty in the coupling variables due to Discipline A affects the outputs of Discipline B which subsequently affects the output of Discipline A. This feedback loop may be difficult to resolve since the mean and variance of the coupling variance may change with each iteration.

Here, we propose to incorporate uncertainty due to coupling variables in the BMDO process; however, we will not address the challenge of resolving coupling variable closure. Instead we will break the coupling loop into a series of disciplinary feedforward loops which may be evaluated in succession. The method improves estimates of the quantity of interest uncertainty but only provides an approximation of the uncertainty due to coupling. A flowchart of the proposed method is shown in Figure 3-1.

The method starts with the closed deterministic coupling variable values at the design point. The uncertainty of the disciplinary outputs is calculated for each discipline, starting with discipline A. Uncertainty due to model discrepancy is applied to the coupling variable outputs of discipline A via Latin Hypercube sampling. This provides the coupling variable inputs from discipline A to discipline B with the as-

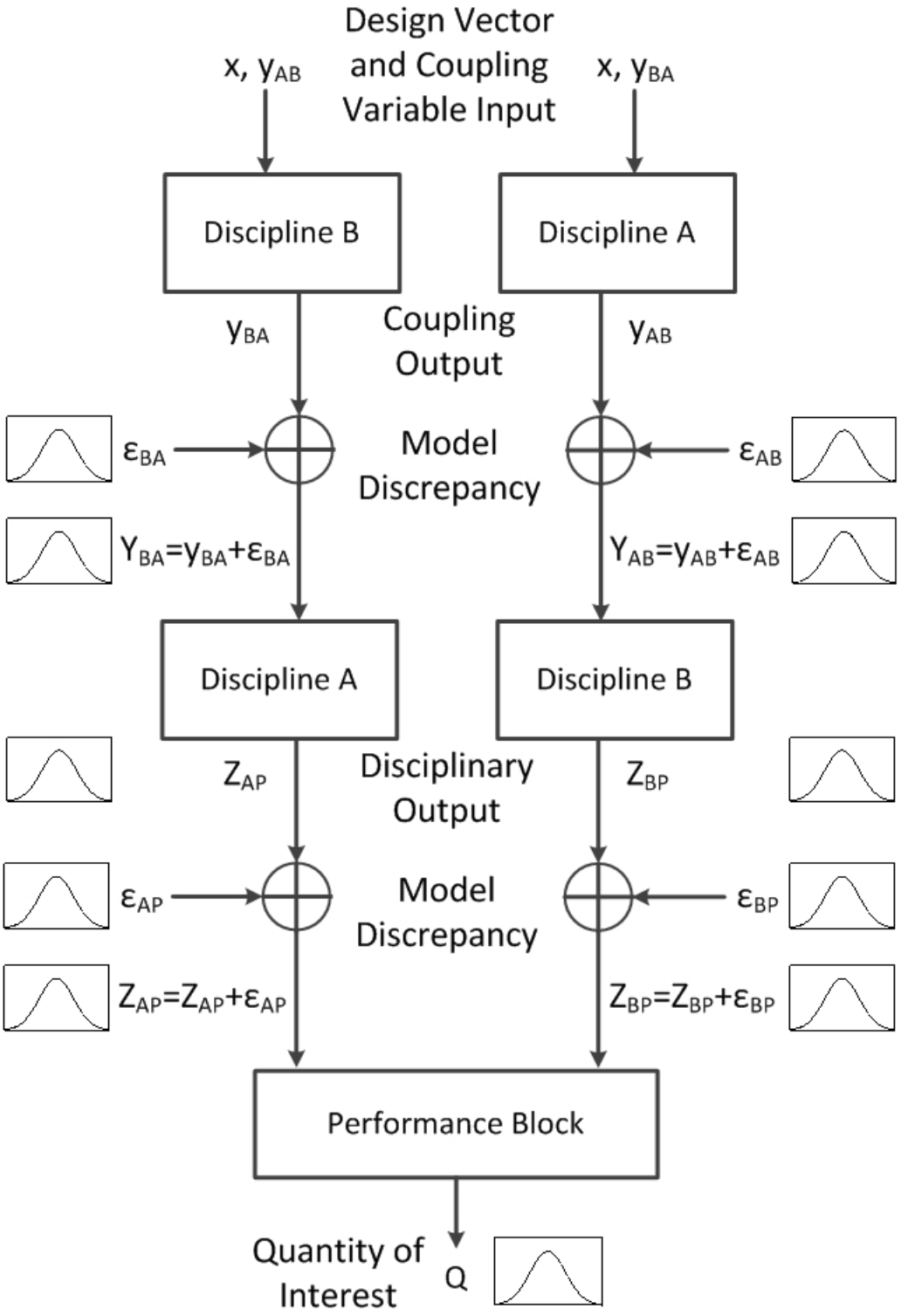

Figure 3-1: Global Sensitivity Analysis Method with Coupling

sociated uncertainty due to discipline A. These samples are then fed into discipline B and evaluated. Model discrepancy due to discipline B is added to the samples, which are then passed back to discipline A. Discipline A is evaluated once more for each sample, model discrepancy due to discipline A is added, and the cycle for discipline A is complete. This cycle is referred to as a "model evaluation cycle". This procedure is repeated for discipline B by switching the role of each discipline in the process. The result of this cycle is an estimate of the disciplinary outputs and associated uncertainty for disciplines A and B with the consideration of uncertainty due to coupling.

Each time model discrepancy is appended, the uncertainty due to model discrepancy is assumed to be normally distributed. No assumptions on the coupling variable distributions are applied during the model evaluation cycle since samples are passed directly between the modules. However, the disciplinary output distributions are assumed to be Gaussian for the information fusion step, prior to the performance block evaluation. It is important to note that this method does not attempt to enforce coupling variable closure. Instead, the goal of this method is to provide an improved estimate of the quantity of interest uncertainty that accounts for the effects of interdisciplinary coupling.

The inclusion of coupling variable uncertainty increases the number of steps in the global sensitivity analysis. Each sample now requires one additional disciplinary evaluation. In addition, resampling now occurs in two locations since the uncertainty is now applied twice for each module—once for the coupling variables and once for the disciplinary output. When calculating the sensitivity indices for discipline A, ϵ_{BA} and ϵ_{BP} must be resampled. Conversely, ϵ_{AB} and ϵ_{AP} must be resampled when calculating the sensitivity indices for discipline B.

3.2 BMDO Walkthrough with Coupling

The walkthrough shown in Section 2.3 is redone with the effects of coupling considered. Coupling does not affect the optimization or evaluation of disciplinary output

uncertainty. As a result, the first two steps of each iteration remains identical to the original walkthrough.

3.2.1 First Iteration

The third step of the first iteration also remains identical to the original walkthrough since no information fusion step occurs due to lack of lower fidelity models.

Step 4: Quantity of Interest Uncertainty

The quantity of interest has a value of 1349 lbm with a standard deviation of 295.2. The mean has decreased by 0.74% but the standard deviation has increased by 9.7% with respect to the results excluding the effects of coupling.

Step 5: Check Termination Criteria

The termination criteria are not satisfied; higher fidelity models exist for both the structures and aeropropulsion modules. The algorithm proceeds onto the next step.

Step 6: Global Sensitivity Analysis

The results of the first global sensitivity analysis are shown in Table 3.1. The main sensitivity index of the structures module has increased slightly from 0.44 to 0.45 and the aeropropulsion module main sensitivity index has decreased from 0.55 to 0.54.

Sensitivity Index	Value
Structures Main	0.45
Aeropropulsion Main	0.54
Structures Total	0.46
Aeropropulsion Total	0.54
Interaction	0.01

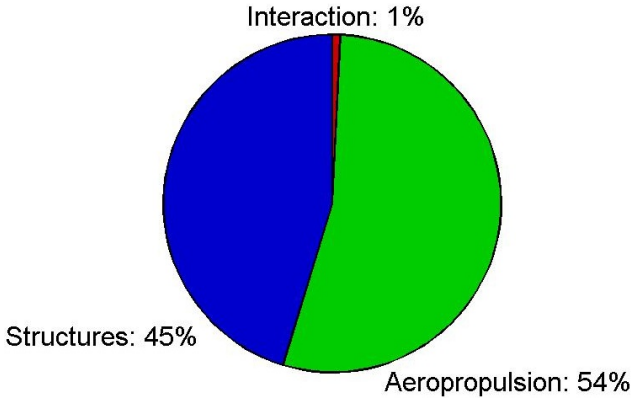

Table 3.1: Results of First Global Sensitivity Analysis with Coupling

The uncertainty due to each discipline was further broken down into its contributing source components: coupling variables and disciplinary output. Table 3.2 shows the sensitivity indices for both sources for each discipline and the interaction sensitivity index. Most of the quantity of interest uncertainty is due to the disciplinary output rather than coupling variables. These values are visualized in Figure 3-2.

Discipline	Source	Sensitivity Index
Structures	Coupling	0.03
Structures	Disciplinary	0.42
Aeropropulsion	Coupling	0.01
Aeropropulsion	Disciplinary	0.53
Both	Interaction	0.01

Table 3.2: Uncertainty breakdown of First Global Sensitivity Analysis with Coupling

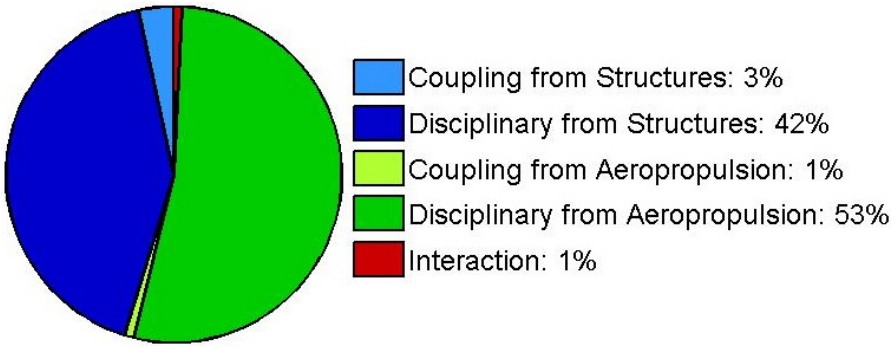

Figure 3-2: Visualization of First Uncertainty Breakdown

Step 7: Increment Model Fidelity

The aeropropulsion module is still the largest contributor to the quantity of interest uncertainty. As a result, the aeropropulsion model fidelity level is incremented to medium while the structures model remains at low fidelity.

3.2.2 Second Iteration

Step 3: Information Fusion

Information fusion is conducted on the disciplinary output distributions after one model evaluation cycle. The results of the information fusion are shown in Table 3.3.

Variable	Units	Low Fidelity	Current Fidelity	Fused Mean
Structures Fidelity	-	Low	Low	-
Aeropropulsion Fidelity	-	Low	Med.	-
Aircraft Weight	lbm	5570	5528	5528
Weight of Fuel On-Board	lbm	2116	2116	2116
Planform Area	ft^2	452.5	452.5	452.5
Cruise TSFC	hr^{-1}	0.112	0.103	0.106
Loiter TSFC	hr^{-1}	0.108	0.102	0.104
Cruise Lift-to-Drag Ratio	-	27.84	27.84	27.84
Loiter Lift-to-Drag Ratio	-	23.24	23.30	23.27
Cruise Lift Coefficient	-	0.989	0.989	0.989
Loiter Lift Coefficient	-	0.980	0.969	0.974

Table 3.3: Results of First Information Fusion with Coupling

Step 4: Quantity of Interest Uncertainty

The quantity of interest has a value of 2129 lbm with a standard deviation of 403.2. The mean has decreased by 0.28% but the standard deviation has increased by 18.6% with respect to the original walkthrough.

Step 5: Check Termination Criteria

The termination criteria are not satisfied; a higher fidelity model exists for the structures module. The algorithm proceeds onto the next step.

Step 6: Global Sensitivity Analysis

The sensitivity indices for the second global sensitivity analysis are shown in Table 3.4. The main sensitivity index of the structures module has decreased slightly from 0.66 to 0.65 and the aeropropulsion module main sensitivity index has increased from 0.33 to 0.34.

Table 3.5 and Figure 3-3 show the results of the disciplinary sensitivity index breakdown for the second iteration. Uncertainty due to the disciplinary output still dominates the overall uncertainty. However, the contributions from the structures modules due to coupling variables has increased over the previous BMDO iteration.

Sensitivity Index	Value
Structures Main	0.65
Aeropropulsion Main	0.34
Structures Total	0.67
Aeropropulsion Total	0.34
Interaction	0.01

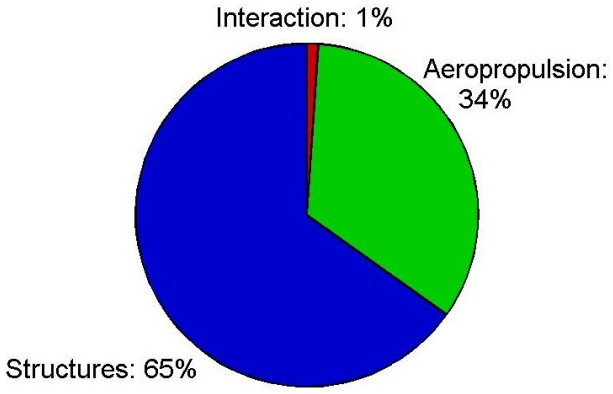

Table 3.4: Results of First Global Sensitivity Analysis with Coupling

Discipline	Source	Sensitivity Index
Structures	Coupling	0.07
Structures	Disciplinary	0.58
Aeropropulsion	Coupling	0.01
Aeropropulsion	Disciplinary	0.34
Both	Interaction	0.01

Table 3.5: Uncertainty breakdown of Second Global Sensitivity Analysis with Coupling

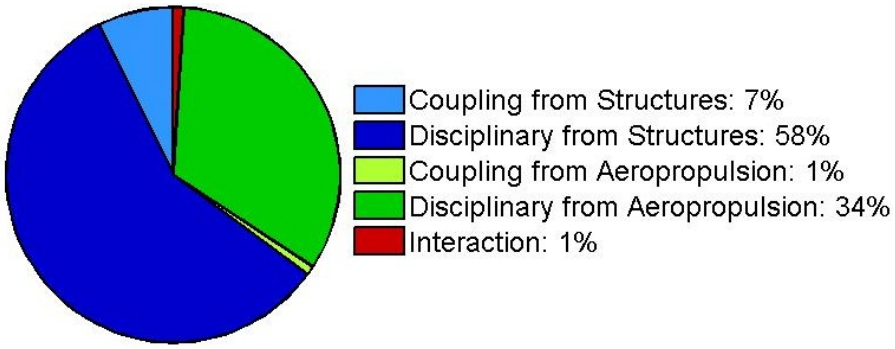

Figure 3-3: Visualization of Second Uncertainty Breakdown

Step 7: Increment Model Fidelity

The structures module is still the largest contributor to the quantity of interest uncertainty. As a result, the structures model fidelity level is incremented to medium while the aeropropulsion model remains at medium fidelity.

3.2.3 Third Iteration

Step 3: Information Fusion

The mean and variance of the disciplinary output are estimated with one model evaluation cycle. The results of the information fusion step on these distributions are shown in Figure 3.3.

Variable	Units	Low Fidelity	Current Fidelity	Fused Mean
Structures Fidelity	-	Low	Med.	-
Aeropropulsion Fidelity	-	Low	Med.	-
Aircraft Weight	lbm	5370	5362	5365
Weight of Fuel On-Board	lbm	1974	2053	2027
Planform Area	ft^2	435.2	435.2	435.2
Cruise TSFC	hr^{-1}	0.113	0.103	0.106
Loiter TSFC	hr^{-1}	0.108	0.105	0.106
Cruise Lift-to-Drag Ratio	-	27.37	27.60	27.53
Loiter Lift-to-Drag Ratio	-	22.99	23.62	23.44
Cruise Lift Coefficient	-	0.991	0.999	0.997
Loiter Lift Coefficient	-	0.976	0.712	0.768

Table 3.6: Results of Second Information Fusion with Coupling

Step 4: Quantity of Interest Uncertainty

The quantity of interest has a value of 2084 lbm with a standard deviation of 268.3. The mean has increased by 0.19% but the standard deviation has increased by 17.3% with respect to the original walkthrough without coupling

Step 5: Check Termination Criteria

The termination criteria are satisfied; neither the structures nor aeropropulsion module have a higher fidelity model available. The algorithm is complete.

3.2.4 Comparison and Interpretation of Results

The results of the BMDO walkthrough with coupling consider show that quantity of interest uncertainty is underestimated if coupling is neglected. This effect becomes

more pronounced when one or more of the disciplines has increased fidelity level. The mean of the quantity of interest was not significantly affected when coupling was considered. The sensitivity indices calculated using the global sensitivity analysis also did not change significantly and no changes were made to the order in which the model fidelities were increased.

Chapter 4

Model Correlation

Correlation is a measure of dependence between two sources of information. Previous research treated models of varying fidelity level as independent information sources. This assumption is relaxed and the effects of model correlation on the BMDO framework are investigated. This chapter discusses the source and importance of correlation. The changes to the basic BMDO method in order to incorporate model correlation are detailed. Two walkthroughs of the BMDO method are completed—one with only model correlation and a second with both model correlation and disciplinary coupling.

4.1 Correlation

The output of models of varying fidelity may exhibit some level of similarity given identical model input. This similarity may come from a variety of sources. Models of different fidelity level may employ identical modeling and/or physics assumptions. Higher fidelity models may simply be an expansion of lower fidelity models by the inclusion of additional physics. Fidelity increases may also be due to the use of denser meshes or tighter convergence tolerances. For these cases, an increase in fidelity level may decrease the uncertainty in the outputs even if the output values do not change significantly. This similarity in model output behavior suggests the models may not be truly independent. Model correlation quantifies the magnitude of this dependence

between the models.

Correlation is estimated by Pearson's correlation coefficient, shown in Equation 4.1. This correlation coefficient measures the degree of linear dependence between two input distributions: A and B. The mean and standard deviation of the inputs are represented by the scalar values μ and σ, respectively.

$$\rho = \frac{E\left[\left(A - \mu_A\right)\left(B - \mu_B\right)\right]}{\sigma_A \sigma_B} \tag{4.1}$$

The correlation between two models may not necessarily be quantified by a single number—it is possible for the correlation coefficient to be a function of the design space. A low fidelity aerodynamics code that assumes an infinite wing may exhibit high correlation with a higher fidelity model that assumes a finite wing if the aspect ratio of the wing is sufficiently high. Conversely, the models may be less correlated if the aspect ratio is small.

Estimation of the correlation coefficient within acceptable confidence bounds at the design points may require a large number of samples. In addition, considerations of sample distribution and the size and shape of the sampling region remain beyond the scope of this research. As a result, several correlation coefficients are selected across a range of values and the consequences of each correlation coefficient on the BMDO process is discussed. This enables the effects of correlation to be investigated without addressing the challenges of estimating the true correlation coefficient.

4.2 Including Correlation in the BMDO Framework

The assumption of independent models has the tendency to underestimate uncertainty, potentially leading to unjustifiable confidence in the design or unreasonably ambitious design decisions. Dependency between the models reduces the total amount of information available to construct the fused distribution. The result is an estimate of the fused distribution that has an increased standard deviation compared to the

case of independent input distributions. When models are correlated, the full reduction in uncertainty possible from independent models cannot be realized. The nature of multifidelity modeling makes the consideration of correlation particularly important since models describing a given discipline are unlikely to be truly uncorrelated.

Reference [4] demonstrates an example of correlated information fusion described in Equations 2.1 and 2.2. This example is reproduced in Figure 4-1 and shows the information fusion step for three different correlation coefficients: 0.0, 0.4, and 0.9. The red distribution has a mean of 2 and standard deviation of 1.0 and represents the lower fidelity model. The blue distribution has a mean and standard deviation of 0.0 and 0.8, respectively, and represents the higher fidelity model. The fused distribution is shown in purple. Note that a taller peak value corresponds to a smaller standard deviation. The plot on the left shows the uncorrelated case. The mean of the fused purple distribution is between the means of the input distributions and the standard deviation is smaller than either of the inputs. The central plot shows the results of the information fusion step with a correlation coefficient of 0.4. The height of the peak has decreased relative to the uncorrelated case, corresponding to an increase in standard deviation of the fused distribution.

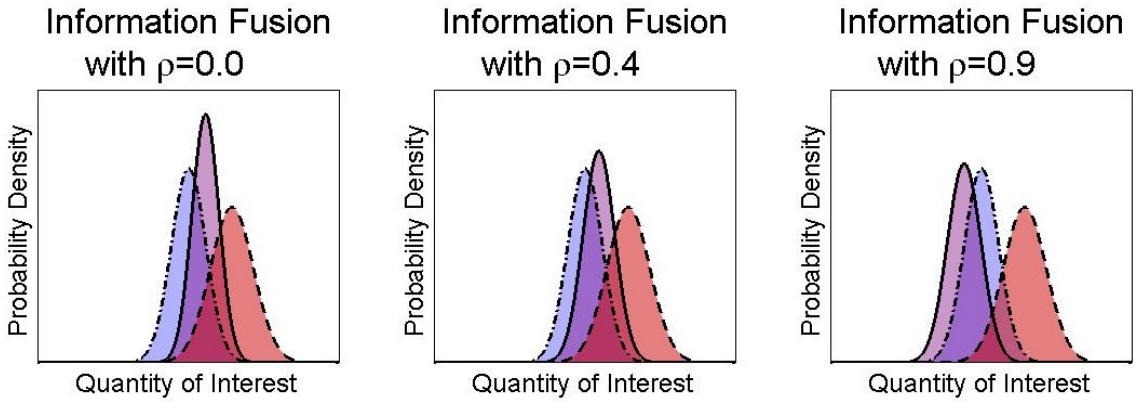

Figure 4-1: Information fusion for inputs with similar variance. The red and blue distributions are the inputs for information fusion and represent lower and higher fidelity models, respectively. The fused distribution is represented via the purple distribution. Results are generated using Equations 2.1 and 2.2

It is possible for the fused mean to lie outside the inputs means when model correlation is sufficiently high, as shown in the right plot of Figure 4-1. This phe-

nomenon is a result of the information fusion equations and is essentially an indirect consideration of model bias. Model Bias is the tendency of the model to under- or overestimate a value of interest with respect to the unknown "true" value. It may also be observed the standard deviation of the strongly correlated case is greater than the previous results with smaller correlation coefficients. This denotes a more conservative estimate of the quantity of interest due to the high similarity between the sources of information.

Figure 4-2 shows the results of the information fusion step for various correlation coefficients with inputs that are more dissimilar [4]. The input red and blue distributions have means of 2.0 and 0.0 and standard deviations of 3.0 and 0.8, respectively. The plot on the left shows the results for uncorrelated information fusion. The standard deviation decreases slightly over the blue (higher fidelity) input distribution. The large standard deviation of the red distribution shows the lower fidelity information source is highly uncertain and may bring only small contributions to the information fusion step. The center plot uses a correlation coefficient of 0.4. The standard deviation of the fused distribution has increased slightly over the uncorrelated case. The rightmost plot employs a correlation coefficient of 0.7. Once again, the mean of the fused distribution is outside the mean values of the inputs.

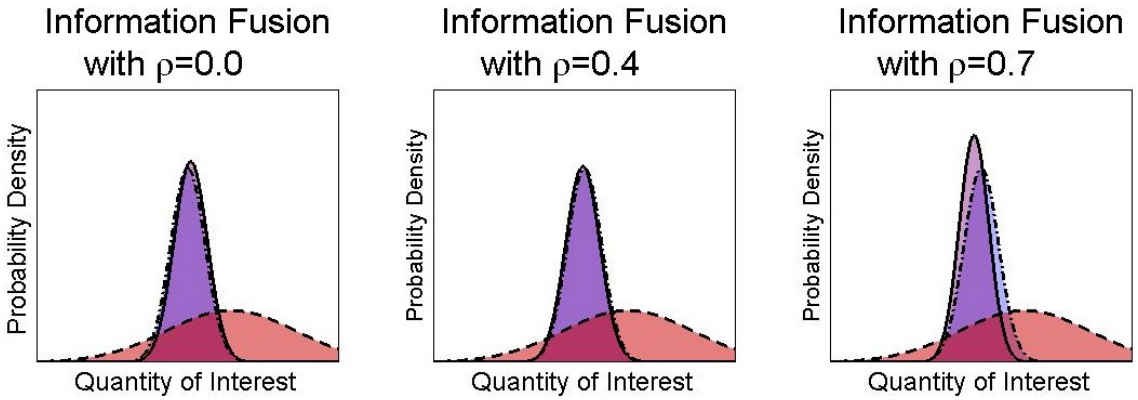

Figure 4-2: Information fusion for inputs with dissimilar variance. The lower and higher fidelity input distributions are shown in red and blue, respectively. Equations 2.1 and 2.2 were used to calculate the fused distribution, shown in purple.

Synthesis Guidelines

The results of the information fusion step with correlation may be summarized:

- Standard deviation of the fused distribution is always smaller than or equal to the standard deviation of the higher fidelity input.
- Fused standard deviation tends to decrease as the standard deviations of the input distributions become more similar.
- Strongly correlated information fusion may result in a fused mean outside the input means.
- The input distribution with the smaller variance is weighted more heavily than inputs with larger variances.

Information fusion may not always provide adequate improvement in the quantity of interest uncertainty to justify the computational expense of the step. This is particularly true if the variance of the input distributions are wildly dissimilar or if the correlation coefficient becomes close to 1.0. In the former, the input with the smaller variance is weighted significantly more heavily in the information fusion step than the input with the larger variance. As a result, the fused distribution may not vary significantly from the input distribution with lower variance and only minor gains may be obtainable. For the latter, a high correlation coefficient indicates the models exhibit strong dependence. As a result, the results of the higher fidelity model should be used as the best estimate of the disciplinary output instead of attempting an information fusion step. The results with correlation coefficients of 0.7 and 0.9 shown in the previous section may be acceptable for those examples, but care should be taken if the correlation coefficient becomes even closer to 1.0.

4.3 BMDO Walkthrough with Correlation

Consideration of model correlation changes not only the information fusion step, but also the subsequent estimation of the quantity of interest uncertainty. The basic

BMDO walkthrough shown in Section 2.3 is repeated with the inclusion model correlation. The results of the first iteration remained unchanged due to the lack of an information fusion step. The updated results of steps 3 and 4 for the second and third iteration are shown below.

4.3.1 Second Iteration

The results of the first information fusion step with correlation are shown in Table 4.1. The third and fourth columns show the mean of the disciplinary outputs calculated from the low and current fidelity models, respectively. The right three columns show the mean values calculated by the information fusion step with three different correlation coefficients: 0.0, 0.4, 0.8. These three correlation coefficient values represent uncorrelated, mildly correlated, and strongly correlated models, respectively.

Variable	Units	Low Fidelity	Current Fidelity	Fusion, $\rho = 0$	Fusion, $\rho = 0.4$	Fusion, $\rho = 0.8$
Structures Fidelity	-	Low	Low	-	-	-
Aeropropulsion Fidelity	-	Low	Med.	-	-	-
Aircraft Weight	lbm	5529	5529	5529	5529	5529
Weight of Fuel On-Board	lbm	2216	2116	2116	2116	2116
Planform Area	ft^2	452.5	452.5	452.5	452.5	452.5
Cruise TSFC	hr^{-1}	0.112	0.103	0.106	0.105	0.101
Loiter TSFC	hr^{-1}	0.113	0.107	0.109	0.108	0.105
Cruise Lift-to-Drag Ratio	-	28.22	28.22	28.22	28.22	28.22
Loiter Lift-to-Drag Ratio	-	23.97	24.02	24.00	24.01	24.03
Cruise Lift Coefficient	-	0.991	0.991	0.991	0.991	0.991
Loiter Lift Coefficient	-	0.623	0.625	0.624	0.624	0.625
Quantity of Interest	lbm	2235	2107	2135	2124	2075
Standard Deviation	lbm	447.9	355.1	339.9	352.9	347.6

Table 4.1: Results of First Information Fusion with Correlation

The standard deviation of the quantity of interest increases from the uncorrelated to mildly correlated case. However, the standard deviation decreases slightly as model correlation becomes stronger for the case when $\rho = 0.8$. As mentioned previously, the information fusion step takes into account bias if the models are strongly correlated. The driving factor in the decrease in standard deviation is likely the TSFC values decreasing below the means of the inputs for these variables.

Depending on the correlation coefficient, the standard deviation for the quantity of interest ranges from 339.9 lbm to 352.9 lbm, an increase up to 3.8% from the results excluding model correlation. The mean of the quantity of interest has decreased up to 2.8% from the uncorrelated BMDO results. This decrease is due to the consideration of model bias for the strongly correlated case.

4.3.2 Third Iteration

The results of the second information fusion step with correlation are shown in Table 4.2. The standard deviation for the quantity of interest exhibits similar behavior to the results of the second iteration. The standard deviation increased from the uncorrelated to mildly correlated case but decreased slightly for the strongly correlated case. This slight decrease in standard is likely due to the fused means for the TSFC values being below the mean values of the inputs.

Variable	Units	Low Fidelity	Current Fidelity	Fusion, $\rho = 0$	Fusion, $\rho = 0.4$	Fusion, $\rho = 0.8$
Structures Fidelity	-	Low	Med.	-	-	-
Aeropropulsion Fidelity	-	Low	Med.	-	-	-
Aircraft Weight	lbm	5328	5358	5349	5352	5365
Weight of Fuel On-Board	lbm	1974	2053	2027	2036	2069
Planform Area	ft^2	435.2	435.2	435.2	435.2	435.2
Cruise TSFC	hr^{-1}	0.112	0.103	0.106	0.105	0.101
Loiter TSFC	hr^{-1}	0.114	0.107	0.109	0.108	0.105
Cruise Lift-to-Drag Ratio	-	27.76	27.76	27.76	27.76	27.76
Loiter Lift-to-Drag Ratio	-	23.83	23.88	23.86	23.87	23.89
Cruise Lift Coefficient	-	0.999	0.999	0.999	0.999	0.999
Loiter Lift Coefficient	-	0.627	0.629	0.628	0.629	0.630
Quantity of Interest	lbm	2175	2055	2081	2071	2024
Standard Deviation	lbm	434.6	273.8	229.5	264.3	264.1

Table 4.2: Results of Second Information Fusion with Correlation

The mean values for the quantity of interest range from 2024 lbm to 2081 lbm, a difference up to 2.7% from the uncorrelated results. The standard deviation ranges from 229.5 lbm to 264.3 lbm for a difference of 15.2%.

4.3.3 Comparison and Interpretation of Results

For our problem, neglecting model correlation may overestimate the mass of fuel burned and underestimate the uncertainty in the quantity of interest. The final estimate of fuel burned during the specified mission has decreased by up to 2.7%. The standard deviation of the quantity of interest has increased up to 15.2%. The magnitude of change from the basic BMDO results is dependent on the value of the correlation coefficient. Differences tend to become more pronounced as:

- Correlation coefficient increases
- The mean values of the inputs become farther apart
- The variance of the input distributions becomes more similar
- More disciplines have lower fidelity models available for information fusion

4.4 BMDO Walkthrough with Coupling and Correlation

The walkthrough of the BMDO algorithm with interdisciplinary coupling shown in Section 3.2 is repeated with the additional effects of model correlation. The first iteration remains identical to previous results due to the lack of an information fusion step.

4.4.1 Second Iteration

The results of the first information fusion step with coupling and correlation is shown in Table 4.3. The mean of the quantity of interest for the strongly correlated case remains below the estimates from the low and current fidelity models.

The mean value of the quantity of interest ranges from 2085 lbm to 2129 lbm, a decrease up to 2.3% from the uncoupled, uncorrelated baseline. The standard deviation has increased from a value of 339.9 lbm from the original BMDO walkthrough to a value ranging from 403.2 lbm to 460.8 lbm, an increase of 18.6 to 35.6%.

Variable	Units	Low Fidelity	Current Fidelity	Fusion, $\rho = 0$	Fusion, $\rho = 0.4$	Fusion, $\rho = 0.8$
Structures Fidelity	-	Low	Low	-	-	-
Aeropropulsion Fidelity	-	Low	Med.	-	-	-
Aircraft Weight	lbm	5570	5528	5528	5528	5528
Weight of Fuel On-Board	lbm	2116	2116	2116	2116	2116
Planform Area	ft^2	452.5	452.5	452.5	452.5	452.5
Cruise TSFC	hr^{-1}	0.112	0.103	0.106	0.105	0.101
Loiter TSFC	hr^{-1}	0.108	0.102	0.104	0.104	0.101
Cruise Lift-to-Drag Ratio	-	27.84	27.84	27.84	27.84	27.83
Loiter Lift-to-Drag Ratio	-	23.24	23.30	23.27	23.28	23.30
Cruise Lift Coefficient	-	0.989	0.989	0.989	0.989	0.989
Loiter Lift Coefficient	-	0.980	0.969	0.974	0.974	0.974
Quantity of Interest	lbm	2248	2097	2129	2124	2085
Standard Deviation	lbm	560.5	461.9	403.2	439.8	460.8

Table 4.3: Results of First Information Fusion with Correlation and Coupling

4.4.2 Third Iteration

Table 4.4 shows the results of the second information fusion step for the coupled, correlated BMDO method. The observations of previous information fusion steps with correlation remain, specifically the quantity of interest mean for the strongly correlated case is smaller than either of the estimates via the low or current fidelity models. The mean TSFC values remain outside the mean of the inputs.

Variable	Units	Low Fidelity	Current Fidelity	Fusion, $\rho = 0$	Fusion, $\rho = 0.4$	Fusion, $\rho = 0.8$
Structures Fidelity	-	Low	Med.	-	-	-
Aeropropulsion Fidelity	-	Low	Med.	-	-	-
Aircraft Weight	lbm	5370	5362	5365	5364	5360
Weight of Fuel On-Board	lbm	1974	2053	2027	2036	2069
Planform Area	ft^2	435.2	435.2	435.2	435.2	435.2
Cruise TSFC	hr^{-1}	0.113	0.103	0.106	0.104	0.100
Loiter TSFC	hr^{-1}	0.108	0.105	0.106	0.106	0.105
Cruise Lift-to-Drag Ratio	-	27.37	27.60	27.53	27.56	27.66
Loiter Lift-to-Drag Ratio	-	22.99	23.62	23.44	23.51	23.79
Cruise Lift Coefficient	-	0.991	0.999	0.997	0.997	1.000
Loiter Lift Coefficient	-	0.976	0.712	0.768	0.731	0.624
Quantity of Interest	lbm	2197	2061	2084	2074	2027
Standard Deviation	lbm	546.8	315.5	268.3	307.2	298.5

Table 4.4: Results of Second Information Fusion with Correlation and Coupling

The standard deviation of the quantity of interest has increased from a baseline value of $229.5\,lbm$ to a value of $268.3 - 307.2\,lbm$ for various correlation coefficients. The estimate of the standard deviations has increased up to 33.9%. The mean of the mass of fuel burned went from $2081\,lbm$ for the baseline value to $2027 - 2084\,lbm$ when correlation and coupling is considered.

The BMDO walkthrough with both interdisciplinary coupling and model correlation has shown the magnitude of quantity of interest uncertainty is significantly underestimated if coupling and correlation are not included in the analysis (up to 35.6%). This increase is larger than the sum of the effects of coupling and correlation independently, suggesting a slight compounding effect. The mean of the quantity of interest is typically less than the estimates from the uncoupled, uncorrelated baseline, but this result may be more problem specific than the underestimation of uncertainty.

Chapter 5

Conclusions

5.1 Summary of Results

The objective of this thesis was to expand the existing Bayesian-based multidisciplinary design optimization method by including interdisciplinary coupling and model correlation. This effort started with an introduction to the basic BMDO method and a detailed discussion of each step of the algorithm. A walkthrough of the method was completed on the problem of interest: the design of a medium-altitude, high-endurance unmanned aerial vehicle.

Interdisciplinary coupling has the potential to create a coupling loop between the disciplines—complicating the estimation of uncertainty. The input for each discipline may no longer be deterministic and the uncertainty associated with the coupling variable may no longer be neglected. The effects of coupling variable uncertainty was estimated by breaking the coupling loop into a series of feedforward loops. The result was an improved estimate of the quantity of interest and its uncertainty. A walkthrough of the BMDO method with coupling was completed, demonstrating the changes to the information fusion and global sensitivity analysis steps of the algorithm.

The nature of multifidelity modeling generally results in disciplinary models that may maintain some level of similarity via underlying physics or applied assumptions. The effect of model correlation on the information fusion step was investigated in

particular and demonstrated with a walkthrough of the BMDO method. In addition, a walkthrough of the BMDO method with both model correlation and coupling was completed.

The results from the previous three chapters have been collected below. Tables 5.1 and 5.2 show the mean and standard deviation values of the quantity of interest at each iteration for the BMDO method with all possible combinations of interdisciplinary coupling and model correlation.

Variable	Units	First Iteration	Second Iteration	Third Iteration
Basic BMDO	*lbm*	1359	2135	2081
BMDO with Coupling	*lbm*	1349	2129	2084
BMDO with Correlation	*lbm*	1359	2075–2135	2024–2081
BMDO with Coupling and Correlation	*lbm*	1349	2085–2129	2027–2084

Table 5.1: Summary of Results: Mean

Variable	Units	First Iteration	Second Iteration	Third Iteration
Basic BMDO	*lbm*	269.2	339.9	229.5
BMDO with Coupling	*lbm*	295.2	403.2	268.3
BMDO with Correlation	*lbm*	269.2	339.9–352.9	229.5–264.3
BMDO with Coupling and Correlation	*lbm*	295.2	403.2–460.8	268.3–307.2

Table 5.2: Summary of Results: Standard Deviation

The changes to the results of the BMDO method become more interesting beyond the first iteration of the BMDO method. The results show the basic BMDO method consistently underestimated the uncertainty in the quantity of interest. Both interdisciplinary coupling and model correlation increased the final uncertainty in the quantity of interest. When both concepts were considered simultaneously, the estimate of quantity of interest uncertainty increased by up to 35.6%.

5.2 Future Work

Four research directions have been identified that may improve the BMDO method. These directions include: optimization, consideration of uncertainty, multifidelity aspects, and handling of coupling and correlation. These topics are discussed individually and exciting research possibilities are identified.

Optimization

Deterministic optimization was used for all work presented here. Uncertainty was estimated and applied after the deterministic optimization. The BMDO method could be improved by incorporating uncertainty into the optimization process. Optimization via decomposition may also prove fruitful due to the multifidelity component of the BMDO method [34]. Decomposition may help preserve information generated as a result of the optimization process. After an iteration of the BMDO method, disciplines that were not increased in fidelity may not need to be re-analyzed. Bilevel Integrated System Synthesis is a decomposition optimization algorithm that may offer such benefits [35].

Uncertainty

Our method of model discrepancy as a portion of the mean had limitations exposed during the BMDO walkthroughs. First, the uncertainty in the quantity of interest should decrease as higher fidelity models are employed. Otherwise, there is little motivation to increase model fidelity only to receive a more uncertain estimate of the quantity of interest. However, the uncertainty increased between the first and second iterations of the BMDO method for each walkthrough. This is simply a result of the mean values of the disciplinary output increasing, corresponding to an increase in uncertainty even as the percentage of the mean that model discrepancy was defined as decreased.

Significant contributions may be made via the use of expert elicitation to improve the estimates of the model discrepancy [6, 7, 10, 38]. Not only would expert elicitation

potentially give more reasonable estimates of uncertainty due to model discrepancy based on the calculations conducted within the models, but the model discrepancy may also become a more complicated function of the discipline's input and output space. Expert elicitation has the potential to create non-Gaussian model discrepancy estimates. As a result, a generalization of the information fusion step for arbitrary distributions may prove beneficial. The use of Sobol' sequences to generate pseudo-random numbers may result in faster convergence of uncertainty and sensitivity index estimates due to a more even distribution of samples than Latin hypercube sampling [36].

Multifidelity Aspects

Additional insight and evidence of the benefits of the BMDO method may be produced if high fidelity models are included. Three sources of information may improve the uncertainty estimates produced by the information fusion step. A multifidelity performance block could also bring forth new questions.

The inclusion of multiple disciplinary models for a given fidelity level may provide interesting results. Depending on the location in the design space, a different model may be more applicable or accurate. The question becomes not only which discipline to increase fidelity level of, but also which model of the desired fidelity level to invoke.

Correlation and Coupling

The consideration of a range of possible correlation coefficients in this research produced a range of possible mean and standard deviation values for the quantity of interest. If the true value of the correlation coefficient could be estimated, then the quantity of interest mean and variance may be quantified more accurately. In addition, estimating the correlation coefficient as a function of the design space could lead to interesting results. Clustering techniques or response surfaces may aid this effort.

Highly correlated models may be used in a manner not considered for this research. If models of different fidelity levels are highly correlated, it may be possible to estimate the output of the higher fidelity model by evaluating the lower fidelity model and

applying a linear regression. A resultant decrease in the computational cost of the BMDO method may be observed. In addition, it is possible for the optimization to direct the design towards a portion of the design space where a model in current use is unnecessarily accurate. In this case, computational resources may be conserved by decreasing the discipline's fidelity level without significantly increasing the quantity of interest uncertainty.

The consideration of more than two disciplines could prove beneficial to the generalization of the BMDO method. The greatest issue with additional disciplines lies in the handling of coupling in the global sensitivity analysis. The number of possible combinations for coupling between disciplines increases and isolating these effects may prove difficult and computationally expensive. The global sensitivity analysis method also assumes coupling variables and disciplinary outputs are independent. The BMDO method could become more rigorous if this assumption is no longer applied. Finally, a method for addressing coupling variable closure would prove valuable to the BMDO method and may further provide a more rigorous analysis of the effects of interdisciplinary coupling.

The sensitivity indices calculated from the global sensitivity analysis are apportioned based on disciplinary contributions to the overall quantity of interest uncertainty. An improved method for calculating sensitivity indices may be to apportion uncertainty in terms of the reduction in uncertainty that may be achieved via an increase in model fidelity level. Such a reformulation would cause the BMDO method to increase the fidelity level of the model with the largest achievable reduction in quantity of interest uncertainty rather than the largest overall contributor to this uncertainty.

Appendix A

Design Vectors

The design variable values for each of the design vectors is shown in Table A.1. The second row of this table denotes the starting design used for optimization to generate the design vector. The coupling variable and disciplinary output values associated with the design vectors are shown in Table A.2.

Variable	Units	Initial	Design 1	Design 2	Design 3
Starting Design	-	-	Initial	Design 1	Design 2
Structures Fidelity Level	-	-	Low	Low	Medium
Aeropropulsion Fidelity Level	-	-	Low	Medium	Medium
Wingspan	ft	98.46	79.43	104.9	100.8
Horizontal Tail Aspect Ratio	-	9.81	8.96	7.91	8.87
Wing Aspect Ratio	-	22.30	29.48	24.32	23.36
Wing Root Station Position	-	0.310	0.304	0.181	0.405
Wing Engine Station Position	-	0.348	0.337	0.357	0.350
Wing Pylon Station Position	-	0.433	0.297	0.290	0.315
Wing Engine Station Chord	-	0.842	0.797	0.902	0.875
Wing Pylon Station Chord	-	0.669	0.804	0.820	0.816
Wing Tip Station Chord	-	0.884	0.535	0.552	0.687
Wing Sweep Angle	deg	3.80	7.22	4.49	2.15
H. Tail Root Station Position	-	0.051	0.566	0.397	0.450
H. Tail Tip Station Chord	-	0.840	0.495	0.434	0.531
H. Tail Sweep Angle	deg	9.60	9.86	12.13	11.04
H. Tail Position	-	0.673	0.746	0.744	0.735
Vert. Tail Aspect Ratio	-	5.21	6.69	4.13	3.11
V. Tail Root Station Position	-	0.593	0.482	0.291	0.497
V. Tail Tip Station Chord	-	0.603	0.550	0.500	0.172
V. Tail Sweep Angle	deg	17.00	8.41	4.35	8.68
V. Tail Position	-	0.528	0.897	0.884	0.988
Wing Fuel Fill Ratio	-	0.194	0.142	0.048	0.068
Fuselage Fuel Fill Ratio	-	0.795	0.693	0.778	0.694
Length of Nose Ratio	ft	18.24	5.45	8.12	12.29
Length of Tail Ratio	ft	16.57	13.28	16.84	21.49
Turbocharger Pressure Ratio	-	3.43	3.74	3.29	3.34
Propeller Radius	m	1.03	1.78	0.689	0.667

Table A.1: Optimized Design Vectors

Variable	Units	Initial	Design 1	Design 2	Design 3
Starting Design	-	-	Initial	Design 1	Design 2
Structures Fidelity Level	-	-	Low	Low	Medium
Aeropropulsion Fidelity Level	-	-	Low	Medium	Medium
Aircraft Weight	lbm	8005	3989	5529	5358
Weight of Fuel On-Board	lbm	3700	1349	2115	2052
Planform Area	ft^2	434.8	214.0	452.5	435.2
Fuselage Wetted Area	ft^2	376.4	208.4	272.7	344.7
H. Tail Planform Area	ft^2	137.3	46.49	124.4	94.97
Root Chord	ft	5.50	3.49	5.40	5.04
Mean Chord	ft	4.42	2.69	4.31	4.32
Position of Center of Gravity	ft	22.73	9.29	12.82	17.12
Position of Neutral Point	ft	23.24	9.39	12.87	17.17
Position of H. Tail	ft	34.76	18.94	25.09	32.31
Engine Weight	lbm	453.8	196.7	244.6	234.5
Cruise Speed	kts	80.35	80.35	80.35	80.35
Dive Speed	kts	58.85	59.21	47.94	48.12
Stall Speed	kts	120.5	120.5	120.5	120.5
Maximum Operating Speed	kts	101.9	102.6	83.03	83.35
Cruise TSFC	hr^{-1}	0.173	0.167	0.103	0.103
Loiter TSFC	hr^{-1}	0.109	0.105	0.107	0.107
Cruise Lift-to-Drag Ratio	-	21.61	22.87	28.21	27.75
Loiter Lift-to-Drag Ratio	-	26.93	30.13	24.02	23.88
Cruise Lift Coefficient	-	0.537	0.543	0.991	0.999
Loiter Lift Coefficient	-	0.928	0.943	0.625	0.629

Table A.2: Coupling Variables and Disciplinary Output at Design Vectors

Bibliography

[1] Abbot, I. and von Doenhoff, A. *Theory of Wing Sections*. Dover Publications, New York, 1959.

[2] Alexandrov, N., Lewis, R., Gumbert, C., Green, L., and Newman, P. Optimization with variable-fidelity models applied to wing design. Technical report, NASA Tech. Rep. CR-209826, December 1999. NASA/CR-2010-216794/VOL2.

[3] Alexandrov, N., Lewis, R., Gumbert, C., Green, L., and Newman, P. Approximation and model management in aerodynamic optimization with variable-fidelity models. *American Institute of Aeronautics and Astronautics*, 38(6):1093–1101, 2001.

[4] Allaire, D., Willcox, K., and Christensen, D. A multifidelity multidisciplinary conceptual design methodology. Ann Arbor, Michigan, July 2011. Presentation at 6th Consortium for Multidisciplinary System Design.

[5] Allaire, D., Willcox, K., and Toupet, O. A Bayesian-based approach to multifidelity multidisciplinary design optimization. Fort Worth, Texas, September 2010. 13th AIAA/ISSMO Multidisciplinary Analysis and Optimization Conference.

[6] Babuscia, A. *Statistical risk estimation for communication system design*. PhD thesis, Massachusetts Institute of Technology, 2012.

[7] Batson, R. and Love, R. Risk analysis approach to transport aircraft technology assessment. *Journal of Aircraft*, 25(2):99–105, 1988.

[8] Booker, A., Dennis Jr., J., Frank, P., Serafini, D., Torczon, V., and Trosset, M. A rigorous framework for optimization of expensive functions by surrogates, 1998.

[9] Choi, S., Alonso, J., and Kroo, I. Two-level multi-fidelity design optimization studies for supersonic jets. *Journal of Aircraft*, 46(3):776–790, 2009.

[10] Clemen, R. and Winkler, R. Combining probability distributions from experts in risk analysis. *Risk Analysis*, 19(2):187–203, 1999.

[11] Corke, T. *Design of Aircraft*. Prentice Hall, Saddle River, New Jersey, 2003.

[12] Deyst, J. The application of estimation theory to managing risk in product developments. Proceedings of the 21st Digital Avionics Systems Conference, Volume 1. pp. 4A3-1-4A3-12, 2002.

[13] Forrester, A. and Keane, A. Recent advances in surrogate-based optimization. *Progress in Aerospace Sciences*, 45:50–79, 2009.

[14] Forrester, A., Keane, A., and Sobester, A. *Engineering Design via Surrogate Modelling: A Practical Guide*. John Wiley and Sons, New York, New York, 2008.

[15] Forrester, S., Sobester, A., and Keane, A. Multi-fidelity optimization via surrogate modelling. *Proceedings of the Royal Society A-Mathematical Physical and Engineering Sciences*, 463(2088):3251–3269, 2007.

[16] Goldstein, M. and Rougier, J. Reified Bayesian modeling and inference for physical systems. *Journal of Statistical Planning and Inference*, 139(3):1221–1239, 2006.

[17] Greitzer, et al. N+3 final report volume 2: Design methodologies for aerodynamics, structures, weight, and thermodynamic cycles. Technical report, Aeronautical Research Council Reports and Memoranda, March 2010. NASA/CR-2010-216794/VOL2.

[18] Homma, T. and Saltelli, A. Importance measures in global sensitivity analysis of nonlinear models. *Reliability Engineering and System Safety*, 52:1–17, 1996.

[19] Jaynes, E. Information theory and statistical mechanics. *The Physical Review*, 106(4):620–630, 1957.

[20] Kennedy, M. and O'Hagan, A. Predicting the output from a complex computer code when fast approximations are available. *Biometrika*, 87(1):1–13, 2000.

[21] Kennedy, M. and O'Hagan, A. Bayesian calibration of computer models. *Royal Statistical Society: Series B*, 63(3):425–464, 2001.

[22] Kennedy, M. O'Hagan, A., and Higgins, N. Bayesian analysis of computer code outputs. *Quantitative Methods for Current Environmental Issues*, pages 227–243, 2002.

[23] Kordonowy, D., Fitzgerald, N., McClellan, J., and Christensen, D. Multifidelity modeling framework for Bayesian-based multidisciplinary aircraft design optimization. Accepted for publication in the 14th AIAA/ISSMO Multidisciplinary Analysis and Optimization Conference, 2012.

[24] Leamer, E. *Specification Searches: Ad Hoc Inference with Nonexperimental Data*. John Wiley and Sons, New York, New York, 1978.

[25] Leary, S., Bhaskar, A., and Keane, A. A knowledge-based approach to response surface modelling in multifidelity optimization. *Journal of Global Optimization*, 26:297–319, 2003.

[26] March, A. *Multifidelity methods for multidisciplinary system design*. PhD thesis, Massachusetts Institute of Technology, 2012.

[27] Park, I., Amarchinta, H., and Grandhi, R. A Bayesian approach for quantification of model uncertainty. *Reliability Engineering & System Safety*, 95(7):777–785, 2010.

[28] Rajnarayan, D., Haas, A., and Kroo, I. Multifidelity gradient-free optimization method and application to aerodynamics design. Victoria, British Columbia, 2008. 12th AIAA/ISSMO Multidisciplinary Analysis and Optimization Conference.

[29] Raymer, D. *Aircraft Design: A Conceptual Approach*. AIAA Education Series. AIAA, 1992.

[30] Reinert, J. and Apostolakis, G. Including model uncertainty in risk-informed decision making. *Annals of Nuclear Energy*, 33(4):354–369, 2006.

[31] Riley, M. and Grandhi, R. Quantification of modeling uncertainty in aeroelastic design. Orlando, Florida, April 2010. 51st AIAA/ASME/ASCE/AHS/ASC Structures, Structural Dynamics, and Materials Conference.

[32] Roskam, J. *Aircraft Design*. DAR Corporation, Lawrence, Kansas, 2000.

[33] Saltelli, A., Ratto, M., Andres, T., Campolongo, F., Cariboni, J., Gatelli, D., Saisana, M., and Tarantola, S. *Global Sensitivity Analysis: The Primer*, pages 155–182. John Wiley and Sons, 2008.

[34] Sobieszczanski-Sobieski, J. Optimization by decomposition: A step from hierarchic to non-hierarchic systems. In Proceedings of the 2nd NASA/Air Force Symposium on Recent Advances in Multidisciplinary Analysis and Optimization, NASA-CP-3031, 1988.

[35] Sobieszczanski-Sobieski, J., Altus, T., Phillips, M., and Sandusky, R. Bilevel integrated system synthesis for concurrent and distributed processing. *American Institute of Aeronautics and Astronautics*, 41(10):1996–2003, 2003.

[36] Sobol', I.M. Uniformly distributed sequences with additional uniformity properties. *USSR Computational Mathematics and Mathematical Physics*, 16(5):236–242, 1976.

[37] Sobol', I.M. Global sensitivity indices for nonlinear mathematical models and their Monte Carlo estimates. *Mathematics and Computers in Simulation*, 55:271–280, 2001.

[38] Tversky, A. and Kahneman, D. Judgement under uncertainty: heuristics and biases. *Science*, 185(4157):1124–1131, 1974.

[39] Winkler, R. Combining probability distributions from dependent information sources. *Decision Analysis*, 24(4):479–488, 1981.

[40] Young, W. *Roark's Formulas for Stress and Strain.* McGraw-Hill, New York, 6th edition, 2000.